## ABSTRACT

# E2F1 regulates an apoptotic response to AKT inhibition in prostate cancer

Kim Su Hwa

Department of Physiology

Seoul National University College of Medicine

The progression of prostate cancer is associated with a selective growth advantage under androgen-depleted conditions, which is accompanied by notorious resistance to most available therapies. Recently geraniol, a naturally occurring monoterpene, has been reported to possess chemotherapeutic potentials against colon and pancreatic cancers. However, the mechanisms of the geraniol action against prostate cancer are poorly understood. In this study, I investigated the anticancer activity of geraniol against prostate cancer.

First, in part Ⅰ, I found that geraniol induces G1 arrest and apoptosis in PC-3 androgen-independent prostate cancer cells. Xenograft model experiments demonstrate that geraniol reduces tumor volumes and weights. In

addition, I showed that geraniol increases the sensitivity of prostate cancer to various chemotherapeutic agents in cultured cells and then demonstrate that the combination of sub-optimal dose of geraniol and docetaxel noticeably suppresses prostate cancer growth in tumor xenograft mice. Next, I investigated the molecular mechanisms of geraniol-induced cell death in PC-3 prostate cancer cells. Among the examined structurally and functionally similar monoterpenes, geraniol specifically induced apoptosis and autophagy. Although independent processes, apoptosis and autophagy acted as cooperative partners to elicit geraniol-induced cell death in PC-3 cells. At a molecular level, geraniol inhibited AKT signaling and activated AMPK signaling, resulting in mTOR inhibition. Combined treatment of AKT inhibitor and AMPK activator markedly suppressed cell growth compared to either treatment alone. My findings provide insight into future investigations that are aimed at elucidating the role of apoptosis and autophagy in prostate cancer therapy and at developing the anticancer strategies deregulating AKT/mTOR pathway.

AKT/mTOR pathway has been reported to possess chemotherapeutic potentials in most of cancers, since PTEN loss and decreased expression of androgen receptor provide activated survival pathway, which confers growth advantages by achieving self-sufficiency in growth signals. However, AKT/mTOR pathway is associated with receptor tyrosine kinase family by negative feedback network. Recent several reports showed that inhibition of AKT/mTOR pathway relieves the negative feedback loop of receptor tyrosine

kinase family. In addition, AKT knockdown did not induce apoptosis, thereby it did not promote profound cell death as a therapeutic approach. Therefore, in part Ⅱ, I used network analysis to assume molecule, which induces synthetic lethality with AKT. As a result of network modeling, I found that E2F1 as a critical hub is down-regulated by high dose of AKT inhibitors. This dose causes significant cell death. In addition I found that inhibition of E2F1 is associated with inhibition of receptor tyrosine kinase family expression and activity. Consequently, I suggest that, in CRPC cells in which achieve growth advantage through hyper-activated oncogenic pathway, combined inhibition of AKT and E2F1 is more effective than either alone.

**Keywords**: Geraniol;AKT;E2F1;Cell death;Prostate cancer

**Student number**: 2007-30968

# CONTENTS

# LIST OF FIGURES

# LIST OF TABLE

# LIST OF ABBREVIATIONS

AR: Androgen receptor

CRPC: Androgen-independent prostate cancer

AMPK: AMP-activated protein kinase

mTOR: mammalian target of rapamycin

PHLPP: PH domain and Leucine rich repeat Protein Phosphatases

PIP3: phosphatidylinositol (3,4,5)- trisphosphate

PIP2: Phosphatidylinositol (4,5)-bisphosphate

CDK: cyclin-dependent kinase

PTEN: Phosphatase and tensin homolog

PI3K: Phosphatidylionositol-3-kinase

GSK3: Glycogen synthase kinase 3

CRPC: Castration resistance prostate cancer

EGFR: Epidermal growth factor receptor

HER: Human Epidermal Growth Factor Receptor

RTK: Receptor tyrosine kinase

IGF-1R: insulin-like growth factor-1 receptor

DEG: Differentially expressed genes

GO: Gene ontology

# I. Introduction

Prostate cancer is the most common noncutaneous cancer and a main cause of cancer death in men (Jemal et al.). Most patients with advanced prostate cancer initially respond to androgen-ablative therapy (Harris et al., 2009). However, the androgen-dependent prostate cancer unavoidably relapses and progresses into the castration-resistance prostate cancer (CRPC) that are currently incurable due to lack of effective treatment regimens (Chen et al., 2004). In addition, the prostate cancer eventually evolves to acquire novel traits: the capability to promote androgen-independent growth and the resistance to other therapeutic options, including chemotherapy (Agus et al., 1999; Chen et al., 2004; Sullivan et al., 1998). Thus, an understanding of the molecular and cellular processes determining tumor traits is an important challenge to develop better therapeutic strategies, and thereby to reduce the burden of prostate cancer.

Prostate cancer cells are reprogrammed to escape from cell cycle arrest and apoptosis under androgen-depleted conditions. Thus, strategies targeting the escape programs to restore the ability to induce cell death are required to improve therapies for prostate cancer. However, cell death is a complex biological phenomenon that is independently or interactively regulated by multiple cellular processes, including apoptosis and autophagy (Lockshin and Zakeri, 2004). Although apoptosis and autophagy share common molecular regulators or pathways, they exhibit synergistic or antagonistic effects on each other during cell death, depending on the cell type

and/or context (Eisenberg-Lerner et al., 2009; Maiuri et al., 2007; Thorburn, 2008). The relationship between apoptosis and autophagy is largely unknown in prostate cancer.

Cell cycle is controlled by the periodic regulation of a number of cell cycle regulators, including cyclins, cyclin-dependent kinases (CDKs), and CDK inhibitory proteins (Hochegger et al., 2008; Malumbres and Barbacid, 2009). Aberrant activity of these regulators confers a limitless replicative potential, a hallmark of cancer (Hanahan and Weinberg, 2000; Luo et al., 2009). In prostate cancer, deregulations or mutations in the cell cycle regulators are frequently observed, which allow the tumor cells to grow under androgen-depleted conditions and eventually stimulate the progression into CRPC (Agus et al., 1999; Karan et al., 2002; LaTulippe et al., 2002). Thus, these observations indicate that controlling cell cycle can be an attractive strategy for prostate cancer therapeutics (Lee et al., 2008; Swanton, 2004). In fact, several small molecule CDK inhibitors are currently undergoing clinical trials for the treatment of patients with prostate cancer (Senderowicz, 2000, 2003; Senderowicz and Sausville, 2000). However, the redundancy of cell cycle regulators and functional complementation among them make it difficult to develop molecularly targeted therapy.

In addition to uncontrolled cell cycle, evading apoptosis is also a hallmark of cancer (Hanahan and Weinberg, 2000; Luo et al., 2009). Small molecule CDK inhibitors have been reported to be able to induce apoptosis in several types of cancer cells (Grant and Roberts, 2003; Senderowicz, 2004).

Although it is unclear whether cell cycle inhibition is causally involved in apoptosis, these observations suggest that cotargeting cell cycle and apoptosis pathways can be an effective strategy for anticancer therapeutics. The deregulation of cell cycle regulators (e.g., cyclins and CDKs) and apoptosis regulators (e.g., Bcl-2 family proteins) is frequently observed in prostate cancer, which can contribute to the progression into CRPC and the development of resistance to therapeutic regimens (Agus et al., 1999; Catz and Johnson, 2003). Indeed, small molecule CDK inhibitors have an effect on lowering therapeutic threshold of conventional anticancer therapies (Grant and Roberts, 2003; Shah and Schwartz, 2000), which suggests that cotargeting cell cycle and apoptosis pathways enhances chemosensitivity.

Aberrant activation of AKT signaling mediates the inhibition of apoptosis and autophagy (Danial and Korsmeyer, 2004; Wang et al., 2003), which may contribute to cancer progression and chemoresistance. In prostate cancer cells, AKT enhances cell survival and increases resistance to cell death under androgen-depleted conditions via various mechanisms, including mTOR activation (Jiao et al., 2007). PTEN, a tumor suppressor gene, antagonizes PI3K activity by dephosphorylating $PIP_3$, which inhibits AKT activity (Hollander et al., 2011). Loss of PTEN has been observed in approximately 70% of metastatic prostate cancer samples (Shen and Abate-Shen, 2007; Taylor et al., 2010), which suggests that PTEN-mediated inhibition of AKT is frequently attenuated in metastatic prostate cancer. In addition, androgen receptor inhibition activates AKT by reducing the

expression level of PHLPP, an AKT phosphatase (Chen et al., 2011). AMPK also interferes with AKT signaling by phosphorylating TSC2 and/or Raptor, which inhibits mTOR activity (Inoki et al., 2003). AMPK inhibition accelerated cell proliferation and promoted malignant behaviors (Zhou et al., 2009). These findings suggest that the biological effects of AKT inhibition may be potentiated by combined treatment with AMPK activator.

Geraniol is a natural acyclic monoterpene derived from herb oils (Ganjewala and Luthra). It is considered as generally recognized as safe (GRAS) by FDA (Lapczynski et al., 2008). It has been shown to possess chemotherapeutic potentials against a few cancer models, such as colon cancer (Carnesecchi et al., 2001) and pancreatic cancer (Wiseman et al., 2007). Therefore, geraniol may be a useful compound that serves as a lead compound for anticancer drug development. In addition, an effort to understand the mechanisms underlying the actions of geraniol can provide insight into novel therapeutic target discovery. However, the molecular mechanisms by which geraniol exerts anticancer activity are poorly understood.

In part 1, I demonstrated that geraniol inhibits prostate cancer growth by inducing cell cycle arrest and apoptosis. The anticancer effect of geraniol was ascertained in *in vitro* culture and *in vivo* xenograft models using PC-3 cell line, a cell model of CRPC. In addition, I found that geraniol enhances the sensitivity of PC-3 cells to chemotherapeutic agents *in vitro* and *in vivo*. Next, I investigated the mechanisms of geraniol action against prostate cancer. I found that geraniol induces apoptosis and autophagy, which function as

cooperative partners to elicit cell death in PC-3 cells. I also showed that geraniol inhibits AKT activity and activates AMPK activity. Combined treatment of AKT inhibitor and AMPK activator markedly suppressed cell growth compared to either treatment alone. Our findings provide insight into future investigations that are aimed at elucidating the role of apoptosis and autophagy in prostate cancer therapy and at developing the anticancer strategies co-targeting AKT and AMPK.

The tumor suppressor PTEN antagonizes PI3K by dephosphorylating $PIP_3$, a key signaling messenger of AKT activation (Stambolic et al., 1998). AKT activity is closely associated with poor clinical outcome in prostate cancer (Kreisberg et al., 2004). Loss of PTEN is observed in approximately 70% of metastatic prostate cancer samples (Shen and Abate-Shen, 2007; Taylor et al., 2010), which increases PI3K-catalyzed $PIP_3$ production and thus activates AKT signaling. PTEN null prostate cancer cells develop androgen-independent phenotypes following castration (Gao et al., 2006; Jiao et al., 2007; Shen and Abate-Shen, 2007; Wang et al., 2003). Androgen receptor plays a critical role in prostate cancer initiation and progression. Androgen receptor (AR) blockade leads to aberrant activation of AKT signaling by impairing AKT phosphatase PHLPP function in PTEN-deficient prostate cancer (Carver et al., 2011; Chen et al., 2011; Mulholland et al., 2011). AKT stimulates survival and development of prostate cancer: AKT deficiency is capable of suppressing prostate cancer development in $PTEN^{+/-}$ mice (Chen et al., 2006). AKT activation promotes the progression to castration-resistant

prostate cancer (Li et al., 2007). These results suggest that AKT activation imparts a survival and growth advantage for these cancer cells in the setting of castration.

Aberrant activation of AKT in prostate cancer has led to an extensive effort to develop targeted therapies (Sarker et al., 2009). However, AKT inhibition often generates conflicting results: small molecule inhibitors or siRNAs against AKT are ineffective in inducing substantial apoptosis without additional proapoptotic insults (Degtyarev et al., 2008). Moreover, AKT inhibition relieves feedback suppression of the receptor tyrosine kinase (RTK) or AR pathway, which limits therapeutic effects of AKT-targeted drugs (Carver et al., 2011; Chandarlapaty et al., 2011).

Relief of negative feedback commonly attenuates the therapeutic response to molecularly targeted anticancer drugs (Ellis and Hicklin, 2009). Therefore, in order for targeted cancer therapies to be effective, it needs to understand what components in a molecular network are involved in feedback regulation. To understand the effect of AKT inhibition in prostate cancer, I computationally analyzed gene expression profiles from PC-3 cells treated with AKT inhibitors.

With advancing recent technology, network modeling is developing predictive therapeutic approach to provide a global view of targeted genes or proteins pathway in tumor biology (Pe'er and Hacohen, 2011). I performed network analysis to identify molecule inducing anti-cancer effects in AKT inhibitors-treated CRPC cells. In this study, network analysis identified E2F1

as a hub protein that is close to AKT. Subsequently, I found that E2F1 suppresses relief of negative feedback of RTK by AKT inhibition. Recent studies reveal that PI3K-AKT signaling blocks E2F1-induced apoptosis through transcriptional programs (Chaussepied and Ginsberg, 2004; Ladu et al., 2008). However, the biological role and its underlying mechanism of E2F1 are unclear in CRPC cells.

In this study, I found that simultaneous targeting of AKT and E2F1 induces significant inhibition of CRPC cells growth. Although AKT inhibition does not induce apoptosis, down-regulated E2F1 suppresses reliefs of feedback network of RTK induced by AKT inhibition. For that reason, these findings identify unexpected actions of E2F1 as a regulator of therapeutic resistance. Together, the results provide novel insight into the prostate cancer biology and therapeutics.

# II. Aims of the study

The advanced prostate cancer eventually acquires a variety of resistances to promote strength on growth signals. PTEN loss has been represented as a strong cause of resistance in CRPC cells, which provide growth advantage by achieving hyper-activated AKT-mTOR pathway.

Thus, in part 1, I employed geraniol as a chemical probe to investigate the anticancer-cellular mechanism of CRPC. In this study, geraniol suppresses prostate cancer growth and exert chemotherapeutic and chemosensitizing activity in CRPC cells. I also showed that geraniol inhibits AKT activity and activates AMPK activity, resulting in inhibition of mTOR activity.

However, recent reports suggest that clinical trials of targeting AKT-mTOR pathway have failed to demonstrated clinical activity due to multiple feedback networks. In addition, targeting AKT-mTOR pathway did not induce significant cell death since it induces autophagy but not apoptosis.

Therefore, in part 2, to understand the effect of AKT inhibition in prostate cancer, in this study, I computationally analyzed gene expression profiles from PC-3 cells treated with AKT inhibitors. Network analysis identified E2F1 as a hub protein that is close to AKT.

# III. Materials and methods

## 3.1 Cell cultures and Reagents

The following cell lines were obtained from ATCC or Korean Cell Line Bank (KCLB): PC-3 (CRPC), DU145 (CRPC), AGS (gastric cancer), Saos-2 (osteosarcoma), MCF7 (breast cancer), HeLa (cervical cancer), HepG2 (hepatocellular carcinoma), A549 (lung adenocarcinoma), and HEK 293 cells. The cells were cultured in RPMI/DMEM media, supplemented with 10% fetal bovine serum and 1% antibiotics. All cell culture agents used were obtained from Hyclone or Gibco. They were maintained in 5% $CO_2$ at 37℃ incubator. Geraniol (Cat. No. 163333), Menthol (Cat. No. 15785), Linalool (Cat. No. L2602), Cineol (Cat. No. C80601), Doxorubicin (Cat. No. D1515), Paclitaxel (Cat. No. T1912), Docetaxel (Cat. No. O1885), Ectoposide (Cat. No. E1383), 5-Fluorouracil (Cat. No. F6627), and Cisplatin (Cat. No. P4394), were purchased from Sigma. Perifosine (Cat. No. S1037) were purchased from Selleck. AKTi-1/2 (Cat. No. 124018) and API-2 (Cat. No. 124012) were purchased from Calbiochem. Perifosine was dissolved in water and all the other reagents were dissolved in DMSO.

## 3.2 MTT assays

PC-3 cells were grown in 12-well or 24-well culture plates (SPL) and each chemical was treated for proper times. After adding 500 μg/ml of 3-(4,5-

Dimethylthiazol-2-yl)-2,5-diphenyltetrazolium bromide (MTT) reagent (Sigma, Cat. No. M5655) into the plates, the cells were incubated in the $CO_2$ incubator for 2 h. Then the culture media and MTT reagent were removed and resulting formazan crystals were dissolved by a proper amount of DMSO. Samples were diluted to proper concentration and were transferred to 96 well plates. The assays were quantified by measuring the absorbance at 570 nm on microplate spectrophotometer (ASYS).

### 3.3 Flow cytometry analysis

PC-3 cells were cultured in 60 mm tissue culture dish. After each chemical treatment, cells were harvested by 300 μl of 1x trypsin-EDTA. After adding 3 ml of culture media, the cells were transferred to 15 ml tube (Falcon). Cell pellets were obtained by centrifugation at 3,000 rpm at 4℃ for 5 min. The supernatant was removed and the cell pellets were resuspended in 1 ml 1X PBS. The cells were transferred to a 1.5 ml tube (Axygen) and were centrifuged at 3,000 rpm at 4℃ for 5 min. The cells pellets were resuspended in 100 μl of 1X Binding Buffer (10 X Annexin V Binding Buffer, BD Biosciences, Cat. No. 556454) at a concentration of 1 X 10e1 cells/ml. After that, the cells were treated with 5 μl of FITC Annexin V (BD Biosciences, Cat. No. 556420). The cells were incubated at room temperature for 15 min. After being incubated, the cells were labeled with propidium iodide solution (50 μg/ml, Sigma, Cat. No. P1740). The cells were transferred to FACS tube

(Falcon Cat. No. 352052) and were analyzed. The percentage of apoptosis induction was measured by flow cytometry (BD Biosciences). ModFitLT V3.0 software was used for data analysis.

### 3.4 Caspase assay

The activity of caspase-3 and -9 from PC-3 cells treated with each chemical was determined in microtiter plates as previously described (Jang et al., 2010). Ac-DEVD-P-nitroaniline and Ac-LEHD-P-nitroaniline (AG scientific) at 2 mM were used fo r caspase-3 and -9 assays, respectively. P-nitroaniline was used to generate the standard curve to evaluate the concentration of the products. A pan-caspase inhibitor zVAD-fmk (Calbioch em) was used to validate the assay method. The absorbance w as measured at 405 nm on microplate spectrophotometer (ASYS).

### 3.5 Assessment of mitochondrial membrane depolarization

Mitochondrial membrane depolarization was evaluated using JC-1 fluorescence probe according to the manufacturer's instructions (Molecular Probes, Cat. No. M34152). PC-3 cells were cultured in 60 mm tissue culture dish. After each chemical treatment, cells were harvested. PC-3 cells were labeled with 2 μM JC-1 for 30 min at 37°C and then analyzed by flow cytometry using 488 nm excitation with 530/30 or 585/42 nm bypass emission filters. The cells without red fluorescence were regarded as the cells

manifesting mitochondrial membrane depolarization.

### 3.6 Whole-Cell Patch Clamp Analysis

HEK 293 cells were seeded in 6-well plates. The following day, 1mg/well pcDNA plasmid vectors containing the cDNA for TRPM8-GFP was transfected into cells using the transfection reagent FuGENE 6 (Roche Molecular Biochemicals) according to the manufacturer's protocol. After 24—48 h, cells were trypsinized and used for whole-cell recording. The whole-cell patch-clamp configuration was used to record membrane currents (voltage clamp), and an Axopatch I-D (Axon Instruments, USA) was used to amplify the currents. The command pulse was applied with an IBM-compatible personal computer and pClamp software (version 6.1; Axon Instruments). Data were filtered at 5 kHz and displayed on an oscilloscope and computer monitor, as well as with a pen recorder (Gould 2200; Gould, Valley View, OH). Results were analyzed with pClamp and Origin software (Microcal Origin version 6.0). For TRPM8 currents, the internal pipette solution for whole cell current recordings contained (in mM) 145 Cs-methanesulfonate, 8 NaCl, 10 Cs-2-bis(2-aminophenoxy)-ethane-N,N,N′,N′-tetraacetic acid(BAPTA) and 10 HEPES-CsOH, adjusted to pH 7.2 with CsOH. The standard extracellular Tyrode's solution contained (in mM) 145 NaCl, 2.8 KCl, 2 CaCl2, 1.2 MgCl2, 10 HEPES, and 10 glucose, adjusted to pH 7.4 with NaOH. The pipette solution contained (in mM) 140 CsCl, 10 HEPES, 0.2 Tris–GTP, 0.5 ethylene glycol-bis-(2-aminoethyl ether)-

N,N,N,N_-tetraacetic acid (EGTA), and 3 Mg–ATP, adjusted to pH 7.3 with CsOH. All experiments were performed at 21─25°C.

### 3.7 Intracellular $Ca^{2+}$ measurement

The detached PC-3 cells were incubated with 5 μM Fura-2-AM in normal Tyrode's solution (10 mM HEPES, 145 mM NaCl, 3.6 mM KCl, 1 mM $MgCl_2$, 1.3 mM $CaCl_2$, and 5 mM glucose) for 30 min at room temperature. After washing twice, the cells were resuspended with normal Tyrode's solution. Fluorescence emission at 510 nm was measured with excitation at 340/380 nm in a stirred quartz-microcuvette of fluorescence spectrophotometer (Photon Technology Instrument). Maximum and minimum fluorescence values at 380 nm ($F_{max}$ and $F_{min}$) were calibrated by addition of 0.2% Triton X-100 and 10 mM EGTA, respectively. The $[Ca^{2+}]_{cyt}$ was calculated from the equation, $[Ca^{2+}] = Kd \times \beta \times (R-R_{min})/(R_{max}-R)$ where $Kd$ is the dissociation constant for Fura-2 (224 nM), β is $F_{min}/F_{max}$, and R is F340/F380.

### 3.8 Quantitative analysis of GFP-LC3 dot

PC-3 cells seeded in 12-well plate were transfected with GFP-LC3 using Fugene-6 (Roche, Cat. No. 11 815 075 001) for 24 h. Then the cells were treated with each chemical for particular time. The cells expressing GFP-LC3 were directly observed by FluoView 1000 confocal microscopy (Olympus). The number of GFP-LC3 dots in each cell (total 30-40 cells) was

counted in at least five independent visual fields.

### 3.9 Xenograft experiment

Balb/C nude mice were subcutaneously inoculated with $1 \times 10^6$ PC-3 cells per mouse in the left inguinal region. To evaluate the anti-tumor activity of geraniol, it was intratumorally treated with the concentrations of 0, 12, 60, or 300 mg/kg. To determine the anti-tumor effect of combination of geraniol with docetaxel, 20 mg/kg geraniol with or without 2 mg/kg docetaxel was intratumorally injected. The tumor size was assessed twice per week using caliper measurements and then the measured values were used to calculate the tumor volume for each individual mouse as previously described as previously described (Noh et al., 2009). Thirty eight days after challenge of PC-3 cells, the mice were sacrificed to measure tumor weight.

### 3.10 RNA isolation and microarray experiments

Total RNA was extracted from PC-3 cells following treatment with vehicle or Perifosine/AKTi-1/2 at 10 uM for 24 h, and then processed according to the manufacturer's guideline (Affymetrix). Human Gene 1.0 ST Array (Affymetrix, GPL6244) was used for gene expression profile analysis.

### 3.11 Network analysis

*Analysis of differentially expressed genes (DEGs).* In order to identifying Perifosine and AKTi perturbed genes, DEGs were extracted. DEGs of Perifosine treated PC-3 cells were determined by using three thresholds; i) log transformed fold-change values (>1.0), ii) p-values of t-test results (<0.01), and iii) expression differences between treated and control sets were larger than thirty (|Expression of treated sample - control sample| > 30.0). After the preparation of DEGs from Perifosine and AKTi treated PC-3 cells, seventy-nine genes were determined as common DEGs of Perifosine and AKTi.

*K-means clustering analysis.* Based on the prepared common seventy-nine DEGs of Perifosine and AKTi, K-means clustering analysis was conducted using MeV ver. 4.7 (PMID: 12613259). Totally, 10 of clusters were analyzed and cluster 7 was selected for further network analysis due to its largest number of genes. Cluster 7 consists of twelve genes as shown in Figure 16C.

*Interaction network building.* Using the twelve genes in cluster 7 and AKT1, I analyzed the interacting neighbors. In this analysis I utilized various biological networks, such as physical or genetic interactions, for the construction of Perifosine and AKTi perturbation related networks. In present study, I used MiMI plugin for Cytoscape (PMID: 18812364) for the analysis of the related networks among query proteins/genes. In addition, a number of resources were accumulated for the building of genetic and physical interactions (PMID 20460452,20093466).

*Bioinformatic analysis*. Number of bioinformatic analysis was

introduced for the identification of enriched pathways and GO terms in presented AKT1 and cluster 7 interacting network using DAVID and BiNGO plugin for Cytoscape. R package (www.r-project.org/) was utilized for the presentation of expression pattern of PTEN and E2F1 using prostate cancer samples of GEO (GSE 3325).

### 3.12 Western blot analysis

PC-3 cells were cultured in either 60 mm or 35 mm tissue culture dish. After each chemical treatment and proper incubation time, cells were harvested and centrifuged at 300 g at 4℃ for 10 min. After discarding supernatant, the crude extracts from PC-3 cell were prepared by incubation with lysis buffer containing 50 mM Tris-HCl (pH 7.4), 150 mM NaCl, 0.5% Triton X-100, 0.5% sodium deoxycholate, 0.1% SDS, 1mM EDTA, protease inhibitor cocktail (Calbiochem, Cat. No. 539134) and phosphatase inhibitor cocktail (Calbiochem, Cat. No. 524625). The lysate was centrifuged for 10 min at 15,000 g and the supernatant was transferred to a new tube. The protein concentration was measured using Bicinchoninic Acid (BCA) method (Thermo, Cat. No. 23223, 23224) according to the BSA (2mg/ml, Biorad, Cat. No. 500-0206) standard curve. Proteins were resolved in 6-15% SDS-PAGE gel and transferred to nitrocellulose membrane (Bio-Rad, Cat. No. 162-0115). Membranes were blocked with 5% skim milk for 1 h, and then incubated with primary antibodies at 4℃ overnight. After washing for 5 min three times with 0.1% TBS-T, blots were exposed to horseradish-peroxidase linked secondary

antibodies at room temperature for 1 h. After washing with 0.1% TBST for 5 min five times, membranes were reacted with SuperSignal west pico solution (Thermo, Cat. No. 34080) and exposed to X-ray film (Agfa). The table below provides detailed information of antibodies. The data shown are representative of at least three independent experiments. The relative intensity of each band was measured using Scion Image software program.

**Table 1.** Experimental conditions used in western blot analysis

| Target protein | Extract amount (μg) | Gel % | 1st antibody | | | | 2nd antibody | | | |
|---|---|---|---|---|---|---|---|---|---|---|
| | | | Company | Cat. No | Titer | Incubation temp&time | Company | Cat. No | Titer | Incubation temp&time |
| Akt | 20 | 10 | cell signaling | #9272 | 1-1000 | 4℃ O/N | cell signaling | 7074 | 1-5000 | RT 1h |
| pAkt (S473) | 20 | 10 | cell signaling | #4058 | 1-1000 | 4℃ O/N | cell signaling | 7074 | 1-5000 | RT 1h |
| pAkt (T308) | 20 | 10 | cell signaling | #4056 | 1-1000 | 4℃ O/N | cell signaling | 7074 | 1-5000 | RT 1h |
| GSK3α/β | 20 | 10 | santa cruz | sc-7291 | 1-500 | 4℃ O/N | Sigma | A-9044 | 1-5000 | RT 1h |
| pGSK3β | 20 | 10 | cell signaling | #9336 | 1-1000 | 4℃ O/N | cell signaling | 7074 | 1-5000 | RT 1h |
| TSC2 | 50 | 6 | cell signaling | #3612 | 1-1000 | 4℃ O/N | cell signaling | 7074 | 1-5000 | RT 1h |
| pTSC2 (T1462) | 50 | 6 | cell signaling | #3611 | 1-1000 | 4℃ O/N | cell signaling | 7074 | 1-5000 | RT 1h |
| mTOR | 20 | 6 | cell signaling | #2972 | 1-1000 | 4℃ O/N | cell signaling | 7074 | 1-5000 | RT 1h |
| pmTOR (S2448) | 20 | 6 | cell signaling | #2971 | 1-1000 | 4℃ O/N | cell signaling | 7074 | 1-5000 | RT 1h |
| p70S6 kinase | 20 | 10 | cell signaling | #9202 | 1-1000 | 4℃ O/N | cell signaling | 7074 | 1-5000 | RT 1h |
| pp70 S6 (T389) | 20 | 10 | cell signaling | #9205 | 1-1000 | 4℃ O/N | cell signaling | 7074 | 1-5000 | RT 1h |
| 4E-BP2 | 20 | 15 | cell signaling | #2845 | 1-1000 | 4℃ O/N | cell signaling | 7074 | 1-5000 | RT 1h |

| | | | | | | | | | | |
|---|---|---|---|---|---|---|---|---|---|---|
| p4E-BP1 (T37/46) | 20 | 15 | cell signaling | #2855 | 1-1000 | 4℃ O/N | cell signaling | 7074 | 1-5000 | RT 1h |
| PDK1 | 20 | 10 | cell signaling | #3062 | 1-1000 | 4℃ O/N | cell signaling | 7074 | 1-5000 | RT 1h |
| pPDK1 (S241) | 20 | 10 | cell signaling | #3061 | 1-1000 | 4℃ O/N | cell signaling | 7074 | 1-5000 | RT 1h |
| AMPKα | 20 | 10 | cell signaling | #2532 | 1-1000 | 4℃ O/N | cell signaling | 7074 | 1-5000 | RT 1h |
| pAMPKα | 20 | 10 | cell signaling | #2535 | 1-1000 | 4℃ O/N | cell signaling | 7074 | 1-5000 | RT 1h |
| ACC | 20 | 6 | cell signaling | #3676 | 1-1000 | 4℃ O/N | cell signaling | 7074 | 1-5000 | RT 1h |
| pACC (S79) | 20 | 6 | cell signaling | #3661 | 1-1000 | 4℃ O/N | cell signaling | 7074 | 1-5000 | RT 1h |
| LC3 | 20 | 15 | MBL | PM036 | 1-1000 | 4℃ O/N | cell signaling | 7074 | 1-5000 | RT 1h |
| CDK1 | 20 | 10 | cell signaling | #9116 | 1-1000 | 4℃ O/N | Sigma | A-9044 | 1-5000 | RT 1h |
| CDK2 | 20 | 10 | santa cruz | sc-163 | 1-500 | 4℃ O/N | cell signaling | 7074 | 1-5000 | RT 1h |
| CDK4 | 20 | 10 | santa cruz | sc-601 | 1-500 | 4℃ O/N | cell signaling | 7074 | 1-5000 | RT 1h |
| CDK6 | 20 | 10 | santa cruz | sc-177 | 1-500 | 4℃ O/N | cell signaling | 7074 | 1-5000 | RT 1h |
| cyclin A | 20 | 10 | santa cruz | sc-751 | 1-500 | 4℃ O/N | cell signaling | 7074 | 1-5000 | RT 1h |
| cyclin B1 | 20 | 10 | santa cruz | sc-752 | 1-500 | 4℃ O/N | cell signaling | 7074 | 1-5000 | RT 1h |
| cyclin D1 | 20 | 10 | cell signaling | #2922 | 1-1000 | 4℃ O/N | cell signaling | 7074 | 1-5000 | RT 1h |
| cyclin E | 20 | 10 | cell signaling | #4129 | 1-1000 | 4℃ O/N | Sigma | A-9044 | 1-5000 | RT 1h |
| p21 | 100 | 15 | santa cruz | sc-6246 | 1-500 | 4℃ O/N | Sigma | A-9044 | 1-5000 | RT 1h |
| p27 | 100 | 15 | santa cruz | sc-1641 | 1-500 | 4℃ O/N | Sigma | A-9044 | 1-5000 | RT 1h |

| | | | | | | | | | | |
|---|---|---|---|---|---|---|---|---|---|---|
| Bcl-2 | 20 | 12 | santa cruz | sc-7382 | 1-500 | 4℃ O/N | Sigma | A-9044 | 1-5000 | RT 1h |
| Bcl-xl | 20 | 12 | cell signaling | #2762 | 1-1000 | 4℃ O/N | cell signaling | 7074 | 1-5000 | RT 1h |
| Bcl-w | 20 | 12 | cell signaling | #2724 | 1-1000 | 4℃ O/N | cell signaling | 7074 | 1-5000 | RT 1h |
| Bax | 20 | 12 | santa cruz | sc-493 | 1-500 | 4℃ O/N | cell signaling | 7074 | 1-5000 | RT 1h |
| Bim | 20 | 12 | cell signaling | #2819 | 1-1000 | 4℃ O/N | cell signaling | 7074 | 1-5000 | RT 1h |
| BNIP3 | 20 | 12 | cell signaling | sc-3769 | 1-1000 | 4℃ O/N | cell signaling | 7074 | 1-5000 | RT 1h |
| Cleaved caspase-3 | 40 | 15 | cell signaling | #9664 | 1-1000 | 4℃ O/N | cell signaling | 7074 | 1-5000 | RT 1h |
| JNK | 20 | 12 | santa cruz | sc-571 | 1-500 | 4℃ O/N | cell signaling | 7074 | 1-5000 | RT 1h |
| pJNK (T183/Y185) | 20 | 12 | cell signaling | #9251 | 1-1000 | 4℃ O/N | cell signaling | 7074 | 1-5000 | RT 1h |
| p38 | 20 | 12 | cell signaling | #9212 | 1-1000 | 4℃ O/N | cell signaling | 7074 | 1-5000 | RT 1h |
| pp38 (T180/Y182) | 20 | 12 | cell signaling | #9216 | 1-1000 | 4℃ O/N | Sigma | A-9044 | 1-5000 | RT 1h |
| p44/42 | 20 | 12 | cell signaling | #9102 | 1-1000 | 4℃ O/N | cell signaling | 7074 | 1-5000 | RT 1h |
| pp44/42 (T202/Y204) | 20 | 12 | cell signaling | #9106 | 1-1000 | 4℃ O/N | Sigma | A-9044 | 1-5000 | RT 1h |
| IGF-IR | 80 | 8 | santa cruz | sc-81464 | 1-500 | 4℃ O/N | Sigma | A-9044 | 1-5000 | RT 1h |
| pIGF-1R | 80 | 8 | Cell signaling | #3024 | 1-1000 | 4℃ O/N | cell signaling | 7074 | 1-5000 | RT 1h |
| pEGFR (Y1173) | 20 | 6 | Cell signaling | #4407 | 1-1000 | 4℃ O/N | cell signaling | 7074 | 1-5000 | RT 1h |
| pEGFR (Y1068) | 20 | 6 | Cell signaling | #2234 | 1-1000 | 4℃ O/N | cell signaling | 7074 | 1-5000 | RT 1h |

| | | | | | | | | | | |
|---|---|---|---|---|---|---|---|---|---|---|
| EGFR | 20 | 6 | Cell signaling | #2232 | 1-1000 | 4℃ O/N | cell signaling | 7074 | 1-5000 | RT 1h |
| pHER2 (Y1221/1222) | 20 | 6 | Cell signaling | #2243 | 1-1000 | 4℃ O/N | cell signaling | 7074 | 1-5000 | RT 1h |
| pHER2 (Y877) | 20 | 6 | Cell signaling | #2241 | 1-1000 | 4℃ O/N | cell signaling | 7074 | 1-5000 | RT 1h |
| HER2 | 20 | 6 | Cell signaling | #2242 | 1-1000 | 4℃ O/N | cell signaling | 7074 | 1-5000 | RT 1h |
| pHER3 (Y1197) | 20 | 6 | Cell signaling | #4561 | 1-1000 | 4℃ O/N | cell signaling | 7074 | 1-5000 | RT 1h |
| pHER3 (Y1289) | 20 | 6 | Cell signaling | #47913 | 1-1000 | 4℃ O/N | cell signaling | 7074 | 1-5000 | RT 1h |
| HER3 | 20 | 6 | Cell signaling | #4754 | 1-1000 | 4℃ O/N | cell signaling | 7074 | 1-5000 | RT 1h |
| GAPDH-HRP | 20 | 10 | santa cruz | sc-20357 | 1-1000 | 4℃ O/N | | | | |

### 3.13 siRNA transfection

PC-3 cells were seeded in 60 mm or 35 mm culture dish. With about 50% confluency, cells were transfected with siRNA mixtures. To prepare siRNA mixture, each siRNA sample and transfection agent, Lipofectamine RNAiMAX reagent (Invitrogen, Cat. No. 13778-150), were diluted in Opti-MEM media (Gibco, Cat. No. 31985) and left in room temperature for 5 min. Then siRNA solution and transfection agent solution were mixed and left for 20 min in room temperature. Suitable volume of the mixture was added to the cells. 4~6 hours after adding transfection mixture, media was changed. 24~72 hours after the transfection, depending on the types of siRNA, cells were treated with chemicals for appropriate times and harvested for further analysis.

siAKT1-5 (Cat. No. SI00299145), siAKT1-10 (Cat. No. SI02757244), siAKT2-7 (Cat. No. SI00287672), siAKT2-6 (Cat. No. SI00299173), siE2F1-5 (Cat. No. SI00300083), siE2F1-6 (Cat. No. SI02664410), siE2F2-4 (Cat. No. SI00375410), siE2F2-2 (Cat. No. SI00375396), and siGFP (Cat. No. 1022064) were purchased from Qiagen (FlextiTube siRNA 5 nmol) and siATG5 (Cat. No. L-004374-00-0005) was purchased from Dharmacon (SMARTpool 5 nmol). All reagents were dissolved in RNase-free water. All reagents were mixed in RNase-free tube (Axygen).

### 3.14 Statistical analysis

All data are expressed as mean ± SEM. Comparison of means among experimental groups was carried out with ANOVA followed by a post hoc test. $P < 0.05$ was considered statistically significant.

# IV. Results

## Part 1

### 1.1 Geraniol suppresses PC-3 cell growth in vitro

Because the anticancer effect of geraniol on prostate cancer has not been examined, we first questioned whether geraniol suppresses PC-3 cell growth. MTT assays showed that cell population gradually decreased in relation to concentrations of geraniol (Fig. 1A). More than 70% of cell population was reduced at 72 h upon geraniol at 1 mM. In addition, I found that geraniol has antitumor activity against a broad spectrum of human cancer cells (Fig. 1B), which suggests that geraniol acts on the common pathways shared among various tumors. However, the anticancer efficacy of geraniol was different depending on the tumor cell types. Among the cell lines tested, Saos-2 cells were found to be relatively resistant to geraniol-induced growth inhibition, compared to other cell lines.

To determine whether geraniol-induced inhibition of tumor cells is resulted from tumor cell death, I performed LDH release assays with PC-3 cells. The increased LDH activity was observed in the cells treated with geraniol in a dose-dependent manner (Fig. 1C). Geraniol at 1 mM caused a 3.5-fold increase of LDH activity in PC-3 cells. These results indicate that geraniol mainly exerts cytotoxic rather than cytostatic effects.

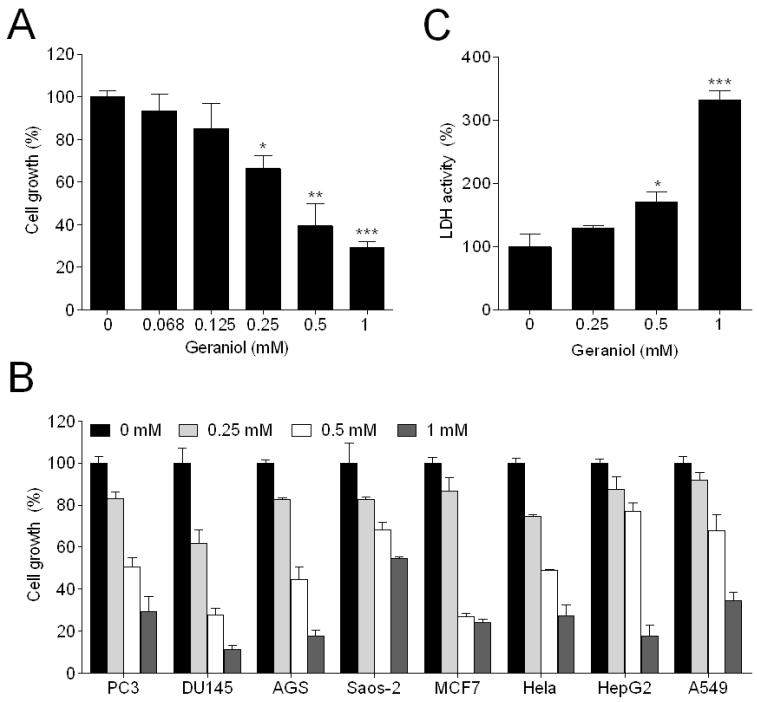


**Fig. 1.** Geraniol has antitumor activity *in vitro*. Various cancer cells were treated with geraniol at the indicated concentrations for 72 h prior to analyses. (A) MTT assays with PC-3 cells. Cell growth is expressed as a relative value to that of the untreated cells which is set to 100%. (B) MTT assays with the various human cancer cells denoted. (C) LDH release assays with PC-3 cells. LDH activity is expressed as a relative value to that of the untreated cells which is set to 100%. The figures show mean ± SEM (n=4).

### 1.2 Geraniol induces cell cycle arrest and apoptosis in PC-3 cells

To determine the cellular processes underlying geraniol-induced growth inhibition of PC-3 cells *in vitro*, I first analyzed the cell cycle profile of PC-3 cells following treatment with geraniol. Flow cytometric analysis showed that the percentage of G1 and/or sub-G1 phase cells was markedly increased in the cells treated with geraniol for 24 h (Fig. 2A) and 48 h (Fig. 2B). These results indicate that geraniol has the ability to induce cell cycle arrest at G1 phase and/or apoptosis.

Because an increase in sub-G1 phase is indicative of apoptosis, I performed caspase-3 activity assay to confirm that geraniol triggers apoptosis. Caspase-3 activity was increased in relation to concentrations of geraniol in PC-3 cells (Fig. 2C), which correlates with the level of cleaved caspase-3, an enzymatically active form (Fig. 2C, inset). I then assessed the mechanisms underlying geraniol-induced apoptosis by examining mitochondria membrane depolarization, an early event of an intrinsic apoptosis signaling. Flow cytometric analysis showed that geraniol noticeably evoked mitochondrial membrane depolarization in a dose-dependent manner in PC-3 cells (Fig. 2D) which demonstrates that geraniol triggers mitochondrial apoptosis pathways. Although geraniol at 0.25 mM caused the mitochondrial membrane depolarization, this change seemed to be insufficient to activate caspase-3 (Fig. 2C and 2D).

To assess the molecular mechanisms underlying the anticancer

activity of geraniol, I analyzed whether geraniol affects the levels of cell cycle and apoptosis regulators using the crude extracts obtained from cultured PC-3 cells. Western blot analysis showed that the expression of four cyclin isotypes (*i.e.*, cyclin A, B, D, and E) and two of CDK family (*i.e.*, CDK1 and CDK4) are reduced in the cells treated with geraniol (Fig. 2E). Contrastingly, the expression of p21 and p27, CDK inhibitory proteins, was markedly elevated under the same condition. In addition, the expression of anti-apoptotic Bcl-2 family members (*i.e.*, Bcl-2 and Bcl-w) was reduced by geraniol, whereas that of pro-apoptotic Bcl-2 family members (*i.e.*, Bax and BNIP3) was elevated. Therefore, our data demonstrate that geraniol inhibits the molecules associated with cell cycle progression and anti-apoptosis and concomitantly activates those with cell cycle pause and pro-apoptosis.

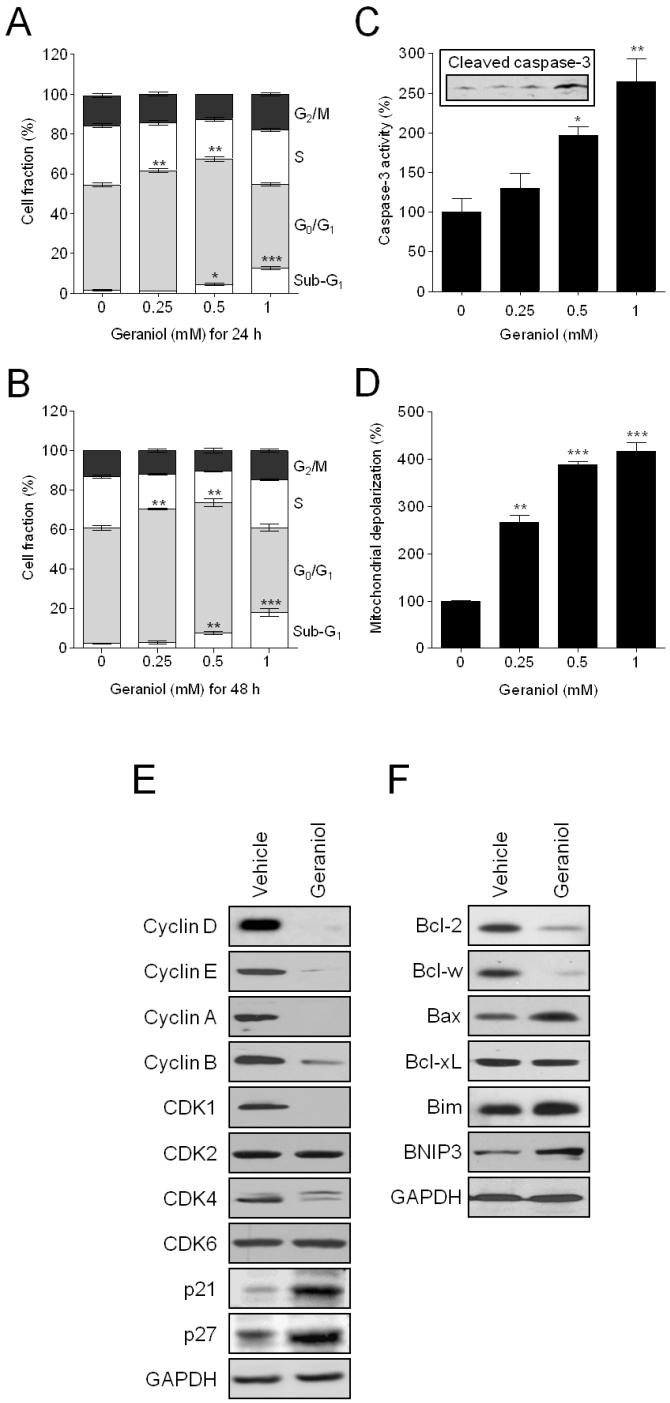
A
Cell fraction (%)
G2/M
S
G0/G1
Sub-G1
Geraniol (mM) for 24 h
B
Geraniol (mM) for 48 h
C
Cleaved caspase-3
Caspase-3 activity (%)
Geraniol (mM)
D
Mitochondrial depolarization (%)
E
Vehicle
Geraniol
Cyclin D
Cyclin E
Cyclin A
Cyclin B
CDK1
CDK2
CDK4
CDK6
p21
p27
GAPDH
F
Bcl-2
Bcl-w
Bax
Bcl-xL
Bim
BNIP3
GAPDH

**Fig. 2.** Geraniol induces cell cycle arrest and apoptosis in PC-3 cells *in vitro*. (A-B) Cell cycle analysis. The cells were treated with geraniol for 24 h (A) or 48 h (B) prior to analyses. Cell fraction is expressed as the percentage of cells in each phase of the cell cycle. The figures show mean ± SEM (n=4). (C) Caspase-3 assays following treatment with geraniol for 48 h. Caspase-3 activity from untreated cells is expressed as 100%. The figures show mean ± SEM (n=6). Cleaved casapase-3 was assessed by western blot analysis (inset). Loading amount was assessed using anti-GAPDH antibody (data not shown) (D) The measurement of mitochondria membrane potential following treatment with geraniol for 48 h. Mitochondria membrane depolarization is expressed as a relative value to that of untreated cells which is set to 100%. The figures show mean ± SEM (n=6). (E-F) Western blot analysis using the indicated antibodies. The crude extracts were prepared from the PC-3 cells treated with geraniol at 1 mM for 24 h. GAPDH was used as a loading control.

### 1.3 Geraniol inhibits PC-3 cell growth in a xenograft model

In order to assure the anticancer activity of geraniol, I performed PC-3 cell xenograft experiments using nude mice. When tumor volumes reached approximately 15 $mm^3$, the mice were intratumorally treated with geraniol at 0, 12, 60, or 300 mg/kg daily. The reduction of tumor volume was obvious in the mice treated with geraniol at 60 or 300 mg/kg (Fig. 3A). In addition, tumor weight decreased in relation to geraniol concentrations (Fig. 3B). These results demonstrate that geraniol effectively suppresses tumor growth *in vivo*.

To determine whether geraniol induces apoptosis tumor cells *in vivo*, I analyzed the percentage of active caspase-3-positive cells and the level of Ki-67, a proliferation marker, using flow cytometry with the cells isolated from the tumor tissues. The percentage of apoptotic cells was elevated in the tumor cells treated with 60 or 300 mg/kg of geraniol (Fig. 3C). On the other hand, the expression level of Ki-67 was reduced in the tumor cells treated with 60 or 300 mg/kg of geraniol (Fig. 3D). These data indicate that geraniol induces apoptosis and cell cycle arrest *in vivo*. These results were corroborated by Western blot analysis. Similarly to the data obtained from cultured cells, the expression of four cyclin isotypes (*i.e.*, cyclin A, B, D, and E), two of CDK family (*i.e.*, CDK1 and CDK4), and Bcl-2 was reduced in the tumor tissues treated with geraniol (Fig. 3E). Contrastingly, the expression of p21, p27, and Bax was markedly elevated in the tumor tissues.

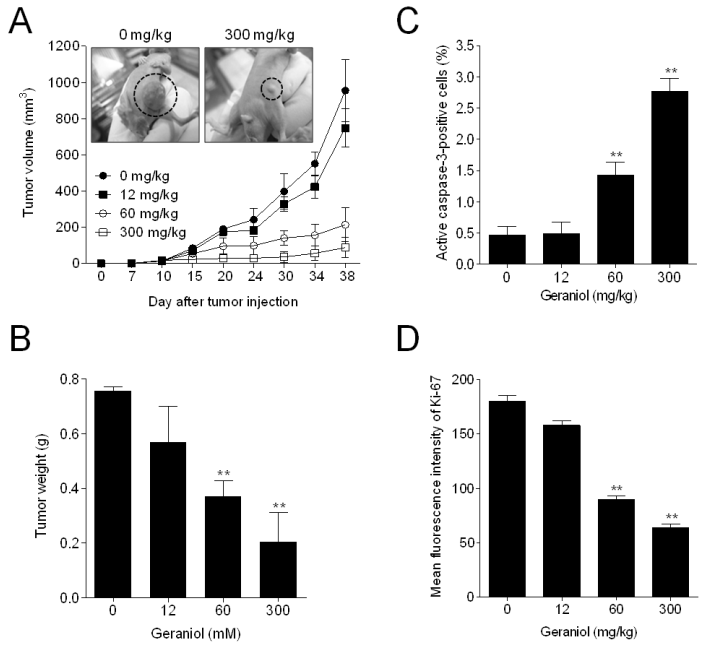
A
0 mg/kg
300 mg/kg
Tumor volume (mm3)
0 mg/kg
12 mg/kg
60 mg/kg
300 mg/kg
Day after tumor injection
B
Tumor weight (g)
Geraniol (mM)
C
Active caspase-3-positive cells (%)
Geraniol (mg/kg)
D
Mean fluorescence intensity of Ki-67
Geraniol (mg/kg)

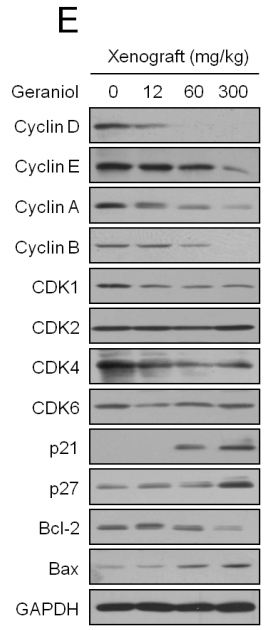
E
Xenograft (mg/kg)
Geraniol 0 12 60 300
Cyclin D
Cyclin E
Cyclin A
Cyclin B
CDK1
CDK2
CDK4
CDK6
p21
p27
Bcl-2
Bax
GAPDH

**Fig. 3.** Geraniol inhibits the growth of PC-3 cells *in vivo*. BALB/c nude mice were subcutaneously inoculated with $1 \times 10^6$ PC-3 cells per each mouse. When tumor volumes reached approximately 15 $mm^3$, the mice were treated with geraniol at the indicated concentrations. (A) Tumor volume analysis. The tumor volumes were recorded twice per week for 38 day. The inset shows the representative photo images. The figures show mean ± SEM (n=4-5) (B) Tumor weight analysis. After 38 days of xenograft implantation, the mice were sacrificed to determine tumor weight. The figures show mean ± SEM (n=4-5) (C) Apoptotic cell assays using PE-conjugated antibody to active caspase-3. The bar graph depicts the percentage of apoptotic cells in the tumor tissues. The figures show mean ± SEM (n=4) (D) Proliferative cell assays using FITC-conjugated antibody to Ki-67. The bar graph represents the mean values of Ki-67 fluorescence intensity in the tumor cells from the tumor tissues. The figures show mean ± SEM (n=4) (E) Western blot analysis using the indicated antibodies. The crude extracts were prepared from the xenografted PC-3 cells treated with geraniol for 38 days. GAPDH was used as a loading control.

## 1.4 Geraniol inhibition of cell growth is independent of TRPM8 calcium channel

Geraniol is structurally related to menthol, an agonist of TRPM8 calcium channel (Fig. 4A). Indeed, geraniol is known to be able to evoke an increase in $[Ca^{2+}]_{cyt}$ (Behrendt et al., 2004). However, it is unclear whether geraniol activates TRPM8 leading to $[Ca^{2+}]_{cyt}$ increase. These factors lead us to determine whether geraniol acts as a TRPM8 agonist and the anticancer effect of geraniol is mediated by TRPM8 activation. To prove whether geraniol acts as a TRPM8 agonist, I performed the whole-cell patch clamp analysis using HEK-293 cells overexpressing TRPM8. An outwardly rectifying current-voltage relationship, a hallmark of TRPM8, was observed in the cells exposed to 1 mM menthol, a known activator of TRPM8 (Fig. 4B). Contrastingly, no TRPM8-specific currents was activated by 1 mM geraniol in the cells overexpressed with TRPM8 (Fig. 4C). These results demonstrate that geraniol does not act as a TRPM8 agonist.

To identify whether geraniol has the ability to induce TRPM8-independent $[Ca^{2+}]_{cyt}$ increase, I measured the effect of geraniol on $[Ca^{2+}]_{cyt}$ in HEK 293 cells, in which TRPM8 is not endogenously expressed (Kim et al., 2009; Mahieu et al., 2007). Geraniol at 1 mM evoked a robust increase in $[Ca^{2+}]_{cyt}$ in HEK-293 cells (Fig. 4D). Additionally, I found that geraniol suppresses the growth of HEK 293 cells in a dose-dependent manner (Fig. 4E), which indicates that TRPM8 is not involved in geraniol-induced growth

inhibition. Furthermore, in PC-3 cells, geraniol evoked a very slight increase in $[Ca^{2+}]_{cyt}$ (Fig. 4F). These results indicate that the anticancer activity of geraniol is unrelated to TRPM8 activation.

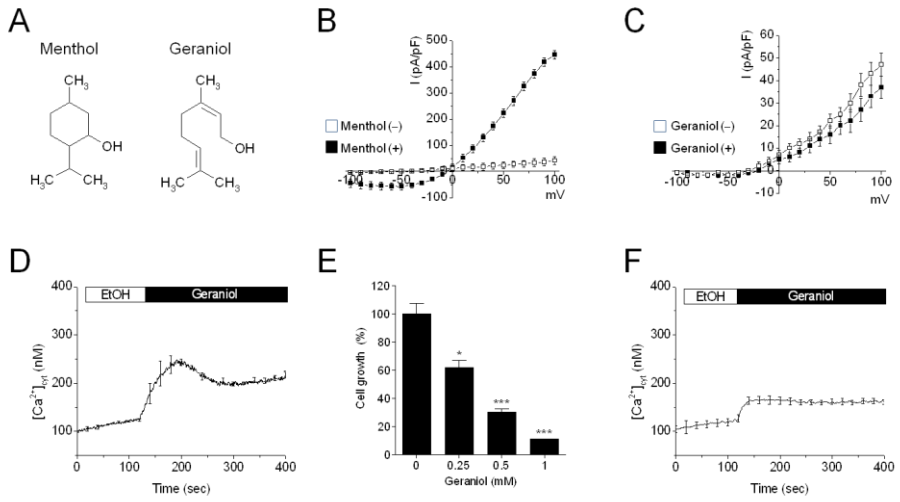


**Fig. 4.** The antitumor activity of geraniol is unrelated to TRPM8 activation. (A) Chemical structures of menthol and geraniol. (B-C) Current-voltage relation (I-V curve) obtained from whole-cell patch clamp analysis. HEK-293 cells overexpressing human TRPM8 was used to determine the electrical responses evoked by 1 mM of menthol or geraniol. The figures show mean ± SEM (n=12). Note the different scales of *y*-axis. (D) The $[Ca^{2+}]_{cyt}$ changes evoked by geraniol at 1 mM were quantitated in empty vector-transfected HEK-293 cells. The figures show mean ± SEM (n=4). (E) MTT assays with empty vector-transfected HEK-293 cells. The figures show mean ± SEM (n=6). (F) The $[Ca^{2+}]_{cyt}$ changes induced by geraniol at 1 mM were determined in PC-3 cells. The figures show mean ± SEM (n=6).

### 1.5 Geraniol increases the chemosensitivity of PC-3 cells *in vitro*

Small molecule CDK inhibitors, which induce cell cycle arrest and apoptosis, are known to have chemosensitizing activity (Grant and Roberts, 2003; Shah and Schwartz, 2000). I thus investigated whether geraniol is able to enhance the sensitivity of PC-3 cells to chemotherapeutic agents. I used doxorubicin, paclitaxel, docetaxel, ectoposide, 5-fluouracil, and cisplatin as chemotherapeutic agents at the indicated sub-toxic concentrations. MTT assays showed that the combination of chemotherapeutic agents with geraniol at 0.25 mM markedly suppressed cell growth, compared to each agent alone (Fig. 5 A-F). This synergistic growth inhibition suggests that geraniol lowers therapeutic threshold of conventional anticancer drugs.

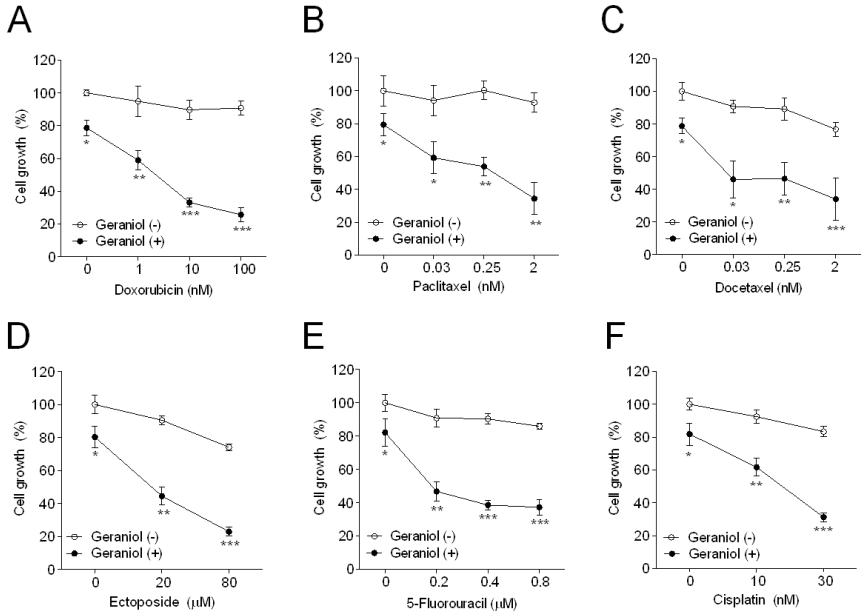


**Fig. 5.** Geraniol increases the chemosensitivity of PC-3 cells *in vitro*. The cells were co-treated with geraniol at 0.25 mM and chemotherapeutic agents, including doxorubicin (A), paclitaxel (B), docetaxel (C), ectoposide (D), 5-fluorouracil (E), and cisplatin (F), at the indicated concentrations prior to MTT assays. The figures show mean ± SEM (n=4).

### 1.6 Geraniol increases the chemosensitivity of PC-3 cells *in vivo*

Because docetaxel is widely used as a chemotherapy agent for CRPC treatment in the clinic, I assessed whether geraniol enhances the sensitivity of PC-3 cells to docetaxel *in vivo*. The nude mice inoculated with PC-3 cells were treated with 20 mg/kg geraniol and/or 2 mg/kg docetaxel. Tumor volumes and weights were noticeably reduced in the group treated with 20 mg/kg of geraniol combined with 2 mg/kg of docetaxel, compared to those groups treated with either alone (Fig. 6A and B). I further analyzed the percentage of active caspase-3-positive cells in the tumor tissues using flow cytometry. As shown in Figure 6C, the percentage of apoptotic cells was remarkably elevated in the tumor tissues treated with the 20 mg/kg of geraniol combined with 2 mg/kg of docetaxel, compared to the tumor tissues treated either alone. Therefore, our data suggest that geraniol lowers therapeutic threshold of conventional anticancer drugs *in vivo*.

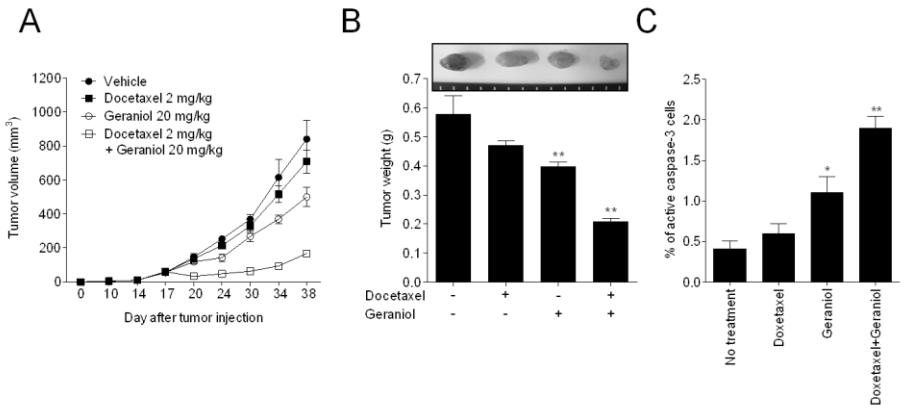


**Fig. 6.** Geraniol increases the chemosensitivity of PC-3 cells *in vivo*. BALB/c nude mice were subcutaneously inoculated with $1 \times 10^6$ PC-3 cells per each mouse. When tumor volumes reached approximately 15 $mm^3$, the mice were treated with 20 mg/kg geraniol and with or without 2 mg/kg docetaxel. (A) Tumor volume analysis. Tumor volumes were recorded twice per week for 38 day. The figures show mean ± SEM (n=5). (B) Tumor weight analysis. The bar graph represents tumor weight 38 day after tumor challenge. The figures show mean ± SEM (n=5). The inset is the representative photo image of tumors (C) Apoptotic cell analysis. The bar graph depicts the percentage of apoptotic PC-3 cells, which is determined using PE-conjugated antibody to active caspase-3.

## 1.7 Geraniol induces apoptosis and autophagy in PC-3 cells

In above study, I found that geraniol induces apoptosis using *in vitro* cultured cells and *in vivo* xenograft models (Kim et al., 2011). Because certain types of monoterpenes, such as menthol, linalool, and cineol, are structurally and functionally similar to geraniol (Behrendt et al., 2004), I compared the anticancer effects of these monoterpenes using MTT assays in PC-3 cells. As presented in Fig. 7A, geraniol significantly suppressed the growth of PC-3 cells compared to other monoterpenes. In addition, the cell cycle profile analysis showed that geraniol potently elevated the percentage of sub-G1 phase cells compared to other monoterpenes (Fig. 7B). Geraniol-specific induction of apoptosis was confirmed using caspase-3 activity assays. Compared to other monoterpenes, geraniol strongly increased caspase-3 activity (Fig. 7C). I also confirmed that geraniol potently produces cleaved caspase-3, an enzymologically active form (Fig. 7D).

Because multiple cellular processes are involved in cell death (Eisenberg-Lerner et al., 2009; Lockshin and Zakeri, 2004), I investigated whether apoptosis is the sole cellular mechanism of geraniol-induced cell death. MTT assays showed that a pan-caspase inhibitor zVAD only partially rescued geraniol-induced cell death (Fig. 8A). These results suggest that geraniol induces other form(s) of cell death in addition to apoptosis.

Based on accumulating, albeit controversial, evidence that autophagy elicits cell death (Codogno and Meijer, 2005; Gozuacik and Kimchi, 2004), I

determined whether geraniol induced cell death via autophagy in addition to apoptosis in PC-3 cells. I first examined the ability of geraniol to induce autophagy by quantifying the number of distinct puncta of GFP-LC3, which is an autophagy marker. When GFP-LC3 puncta were counted in each cell, the number of puncta markedly increased in geraniol-treated cells (Fig. 8B and 8C). Western blot analysis showed that geraniol increased the level of LC3-II, which is a biomarker of autophagy (Fig. 8D). Pepstatin A and E64D, which are lyosomal protease inhibitors, further increased the level of LC3-II (Fig. 8D). I also observed that increased expression levels of ATG5, which is a key protein of autophagy, correlated with increasing concentrations of geraniol (Fig. 8D). I examined the specificity of geraniol action on autophagy in PC-3 cells. Among the monoterpenes, geraniol potently increased the number of GFP-LC3 puncta and the level of LC-3 II (Fig. 8E). Although menthol slightly increased the number of GFP-LC3 puncta, it did not affect the level of LC-3 II. These results demonstrate that geraniol specifically induces autophagy in PC-3 cells.

To examine which process was activated first, I performed a time-course analysis of autophagy and apoptosis in geraniol-treated PC-3 cells. LC-3 II and ATG5 levels were elevated following treatment with geraniol for 12 h, and were reduced after 48 h (Fig. 8F). Alterations in the levels of proapoptotic (cleaved caspase-3 and Bax) and antiapoptotic proteins (Bcl-xL) were observed after 48 h of geraniol treatment (Fig. 8F). Therefore, our results indicate that autophagy is initiated before apoptosis in geraniol-treated PC-3

cells. Although Bcl-2 exerts both antiapoptotic and antiautophagic function (Levine et al., 2008), our results show that geraniol induces autophagy before reduction of Bcl-2 level, suggesting that Bcl-2 is not a main factor of geraniol-induced autophagy. On the contrary, Bcl-2 level inversely well correlated with cleaved caspase-3 and Bax.

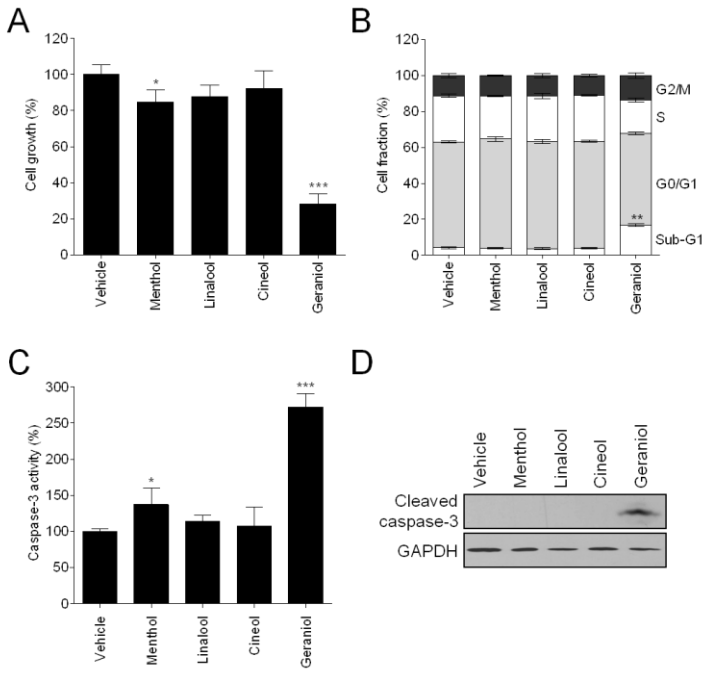


**Figure 7.** Geraniol induces apoptosis in PC-3 cells. (A) The cells were treated with the indicated monoterpenes (1 mM each) for 72 h prior to MTT assays. Cell growth was expressed as a relative absorbance value compared to that of vehicle-treated cells which was set to 100%. (B) The cells were treated with the monterpenes (1 mM each) for 20 h prior to cell cycle analyses. The cell fraction was expressed as the percentage of each phase of the cell cycle. (C) The cells were incubated with the monoterpenes (1 mM each) for 48 h prior to caspase-3 activity assays. Caspase-3 activity in vehicle-treated cells was expressed as 100%. (D) The cells were incubated with the monoterpenes (1 mM each) 60 h prior to Western blot analyses. Equal loading was ascertained based on GAPDH levels. The data were expressed as the mean ± SEM (n=4). * $P < 0.05$, ** $P < 0.01$, *** $P < 0.005$.

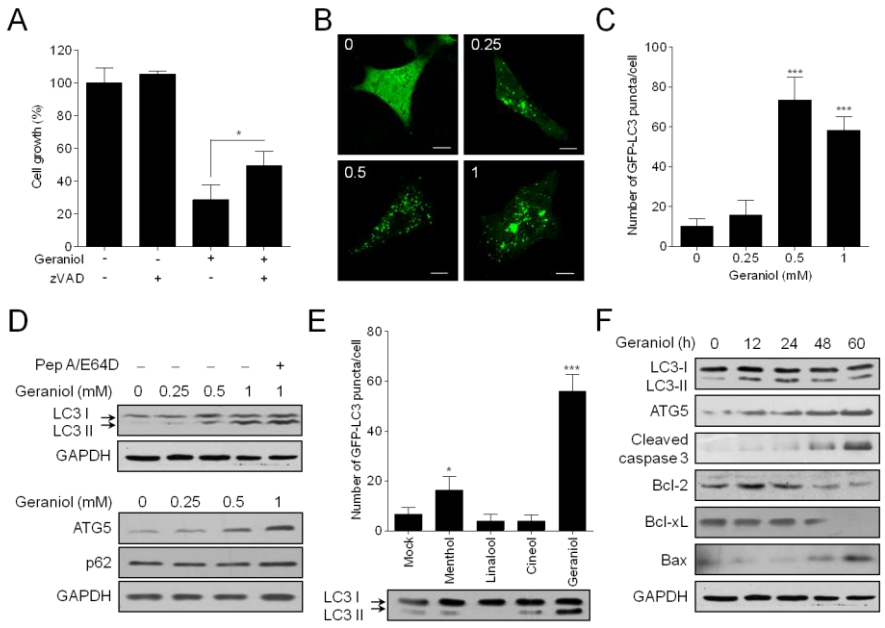


**Figure 8.** Geraniol induces autophagy in PC-3 cells. (A) The cells were treated with geraniol (1 mM) and/or zVAD (10 μM) for 72 h prior to MTT assays. The data were expressed as the mean ± SEM (n=4). * $P < 0.05$. (B and C) The cells expressing GFP-LC3 were treated with geraniol at the indicated concentrations for 20 h prior to confocal microscopic analyses. The number of GFP-LC3 dots in each cell was counted in at least three independent visual fields. The data were expressed as the mean ± SEM (n=20). *** $P < 0.005$. (D) The cells were treated with geraniol at the indicated concentrations for 20 h and LC3-II level were determined using Western blot analysis. (E) The cells expressing GFP-LC3 were incubated with the monoterpenes (1 mM each) for 20 h prior to counting the number of GFP-LC3 puncta. The data were expressed as the mean ± SEM (n=20). * $P < 0.05$, *** $P < 0.005$. (F) The cells were treated with geraniol at 1 mM for the indicated times.

## 1.8 Geraniol-induced apoptosis and autophagy cooperate to elicit cell death in PC-3 cells

Because apoptosis is not the sole cell death mechanism in geraniol-treated PC-3 cells (Fig. 7C), I assessed the significance of autophagy in geraniol-induced cell death. Treatment with zVAD or 3-MA (an autophagy blocker) alone partially rescued geraniol-induced cell death, whereas the combined treatment of zVAD and 3-MA restored cell growth up to 85% (Fig. 9A). When siRNA against ATG5 (siATG5) was used instead of 3-MA, I observed that the combined treatment of zVAD and siATG5 markedly restored cell growth compared to either treatment alone (Fig. 9B). These results indicate that apoptosis and autophagy cooperate to cause cell death in geraniol-treated cells.

I examined the inter-relationship between apoptosis and autophagy in geraniol-induced cell death. Inhibition of autophagy using 3-MA did not affect apoptosis, which was determined using caspase-3 activity assays (Fig. 9C). Inhibition of apoptosis using zVAD did not alter autophagy, which was measured using GFP-LC3 puncta formation assays (Fig. 9D). These results suggest that autophagy and apoptosis occur independently of each other in geraniol-treated PC-3 cells. However, these processes functioned as cooperative partners to induce cell death.

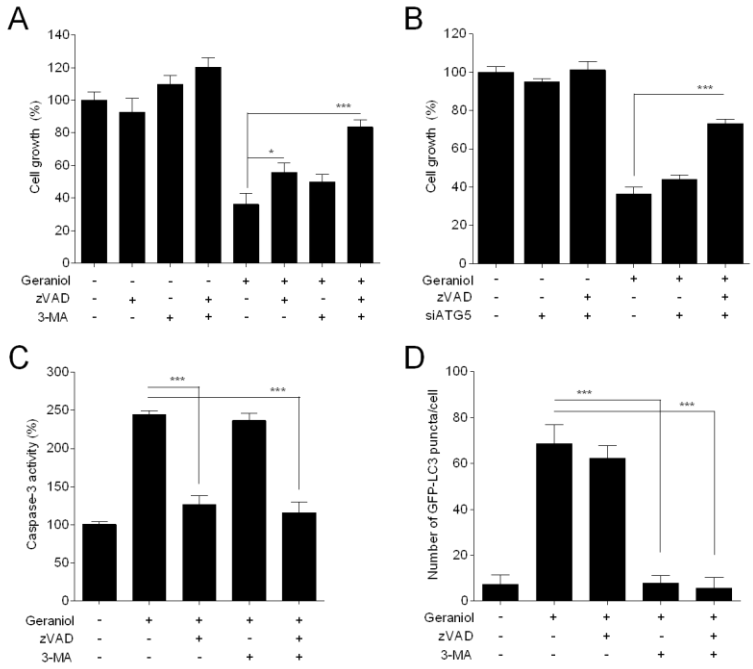


**Figure 9.** Combined inhibition of apoptosis and autophagy restores cell growth in PC-3 cells. (A) The cells were treated with geraniol (1 mM), zVAD (10 μM), and/or 3-MA (2 mM) for 72 h. Cell growth was expressed as a relative value compared to the untreated cells. The data were expressed as the mean ± SEM (n=4). (B) The cells were treated with geraniol (1 mM), zVAD (10 μM), and/or siATG5 (50 nM) for 72 h prior to MTT assays. The data were expressed as the ± SEM (n=4). (C) The cells were incubated with geraniol (1 mM), zVAD (10 μM), and/or 3-MA (2 mM) for 48 h prior to caspase-3 activity assay. The data were expressed as the mean ± SEM (n=4). (D) The cells were incubated with geraniol (1 mM), zVAD (10 μM), and/or 3-MA (2 mM) for 20 h prior to quantifying the number of GFP-LC3 puncta. The data were expressed as the mean ± SEM (n=20). * $P < 0.05$, *** $P < 0.005$.

### 1.11 The effects of geraniol is unrelated to HMG-CoA reductase and TRPM8 pathways in PC-3 cells

Geraniol inhibits the activity of HMG-CoA reductase, which catalyzes the production of mevalonate from HMG-CoA (Yu et al., 1995). Therefore, I tested whether mevalonate deficiency is attributable for geraniol-induced cell death. MTT assays showed that mevalonate supplementation to the culture medium did not rescue geraniol-induced cell death (Fig. 10).

Certain types of monoterpenes have agonistic activity for the TRPM8 calcium channel (Behrendt et al., 2004). To examine the involvement of TRPM8 in geraniol-induced cell death, I performed whole-cell patch clamp analysis in TRPM8-transfected HEK 293 cells. Only menthol evoked TRPM8 current (Fig. 11A), whereas other monoterpenes did not act as TRPM8 agonists (Fig. 11B-D). In addition, compared to other monoterpenes (Fig. 11E-G), geraniol the most weakly elevated cytoplasmic calcium levels (Fig. 11H). Because linalool, cineol, or geraniol is not a TRPM8 agonist, our results suggest that these monoterpenes elevate cytoplasmic calcium levels increased via TRPM8-independent mechanisms. Taken together, these results suggest that geraniol-induced cell death is not mediated by mevalonate deficiency and TRPM8 activation.

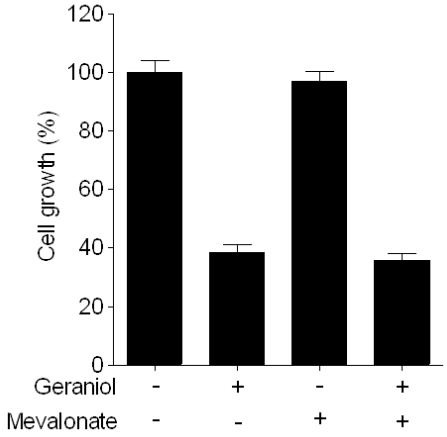


**Figure 10**. Mevalonate supplementation does not rescue geraniol-induced cell death in PC-3 cells. The cells were treated with geraniol (1 mM) and/or mevalonate (500 μM) for 72 h prior to MTT assays. Cell growth was expressed as a relative value compared to that of the untreated cells which was set to 100%. The data were expressed as the mean ± SEM (n=4).

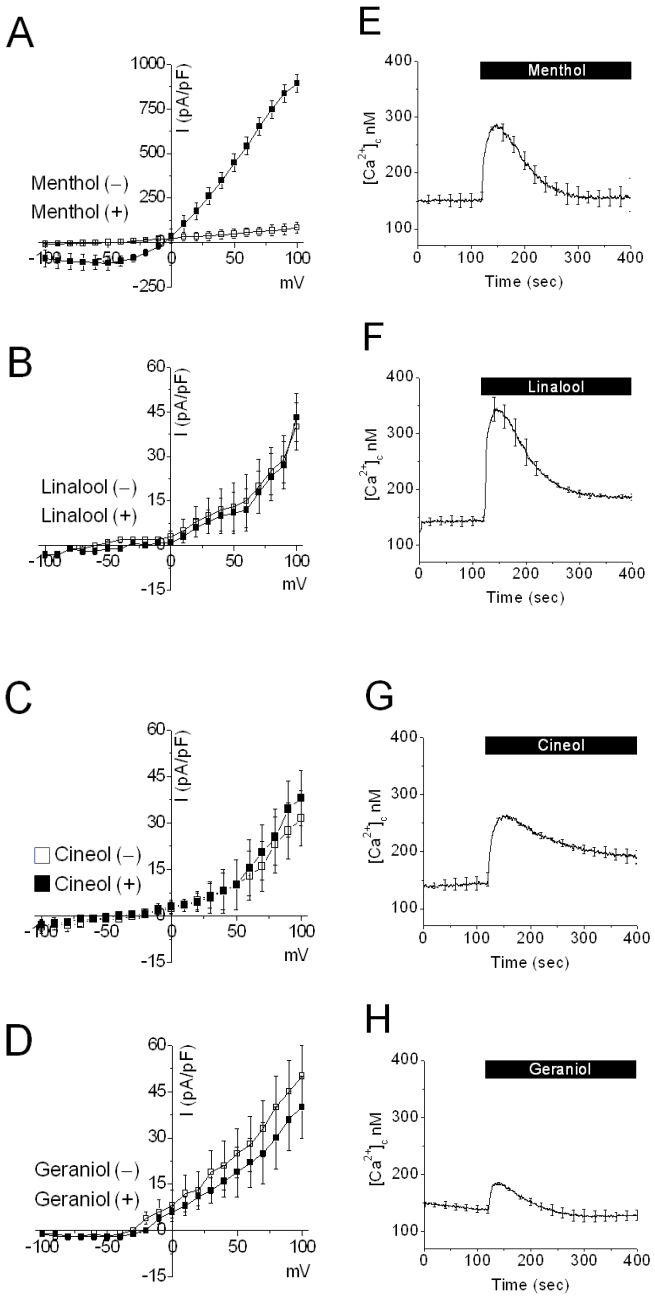
A
B
C
D
E
F
G
H
I (pA/pF)
mV
Menthol (–)
Menthol (+)
Linalool (–)
Linalool (+)
Cineol (–)
Cineol (+)
Geraniol (–)
Geraniol (+)
Menthol
Linalool
Cineol
Geraniol
[Ca2+]c nM
Time (sec)

**Figure 11**. TRPM8 activation is not involved in geraniol-induced cell death in PC-3 cells. (A-D) The HEK 293 cells overexpressing human TRPM8 were used to evaluate change in the current-voltage relationship following treatment with the indicated monoterpenes (1 mM each). Note the different scales of the y-axes. The data were expressed as the mean ± SEM (n=12). (E-H) The cytoplasmic calcium concentration was measured using Fura-2-AM dye in PC-3 cells that were treated with monoterpene (1 mM each). The data were expressed as the mean ± SEM (n=12).

### 1.11 Geraniol inhibits AKT-mTOR signaling in PC-3 cells

Aberrant activation of AKT and mTOR following PTEN loss and/or androgen receptor inhibition has been observed in prostate cancer (Mulholland et al., 2011; Taylor et al., 2010) and mediates the inhibition of apoptosis and autophagy (Danial and Korsmeyer, 2004; Wang et al., 2003). Therefore, I investigated whether geraniol inhibited AKT-mTOR signaling. As shown in Fig. 12A, geraniol inhibited AKT and its downstream effectors, including mTOR, S6K, and 4EBP, in a concentration-dependent manner. In addition, geraniol specifically inhibited AKT/mTOR signaling compared to cineol (data not shown). AKT inhibition was observed following treatment with geraniol for 1 h and was sustained thereafter (Fig. 12B). However, geraniol did not activate MAP kinases, including ERK, JNK, and p38 kinase (Fig. 12C).

I examined the mechanisms by which geraniol reduced AKT phosphorylation. I demonstrated that geraniol did not inhibit the phosphorylation of PDK1, which is an AKT upstream kinase (Fig. 12D). I investigated whether phosphatase pathways were involved in geraniol-induced AKT inhibition. Okadaic acid, which is a PP2A inhibitor, completely restored AKT phosphorylation compared to tautomycin, which is a PP1 inhibitor, in geraniol-treated cells (Fig. 12E). These results indicate that geraniol inhibits AKT signaling via regulation of the PP2A pathways.

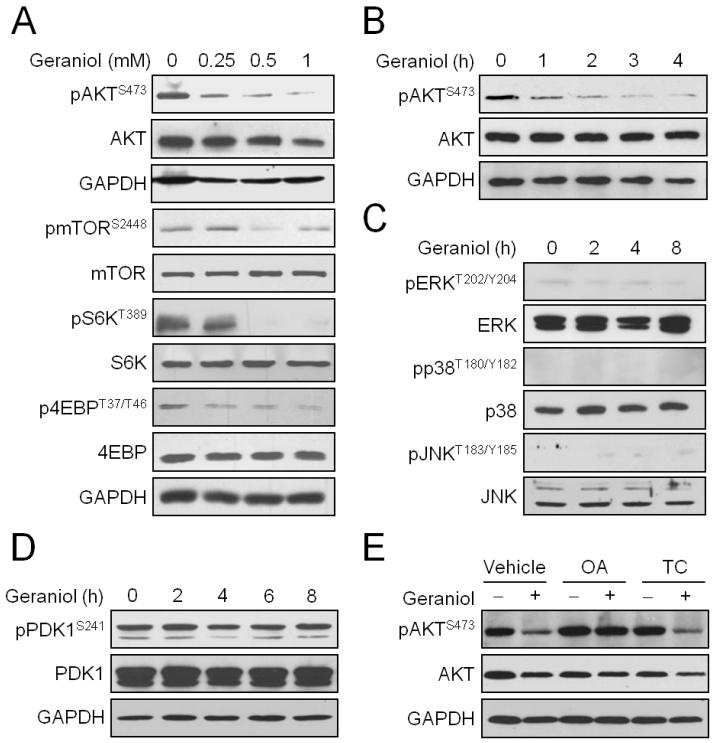


**Figure 12.** Geraniol inhibits the AKT-mTOR pathway in PC-3 cells. (A) The cells were treated with geraniol at the indicated concentrations for 4 h prior to Western blot analyses. (B-D) The cells were incubated with geraniol (1 mM) for the indicated times. (E) The cells were pretreated with okadaic acid (OA, 100 nM), or tautomycin (TC, 500 nM) for 30 min followed by treatment with geraniol (1 mM) for 4 h.

### 1.12 Geraniol activates AMPK signaling in PC-3 cells

Because mTOR activity is also inhibited by AMPK signaling (Inoki et al., 2003), I examined whether geraniol activates AMPK. Compared to cineol, geraniol activated AMPK and increased the phosphorylation of ACC, an AMPK substrate (Fig. 13A). These results indicate that geraniol inhibits mTOR pathways by inhibiting AKT and activating AMPK signaling.

Either AKT inhibition or AMPK activation suppresses prostate cancer growth (Zhou et al., 2009). Therefore, I investigated whether the combined modulation of AKT and AMPK is more effective than either alone in prostate cancer therapy. MTT assays showed that combined treatment of perifosine (an AKT inhibitor) and AICAR (an AMPK activator) markedly suppressed cell growth compared to either treatment alone (Fig 13B). In addition, AICAR enhanced the anticancer activities of several AKT inhibitors at sub-optimal doses (Fig. 13C). These results indicate that the concurrent modulation of AKT and AMPK activities may be a promising strategy for prostate cancer treatment.

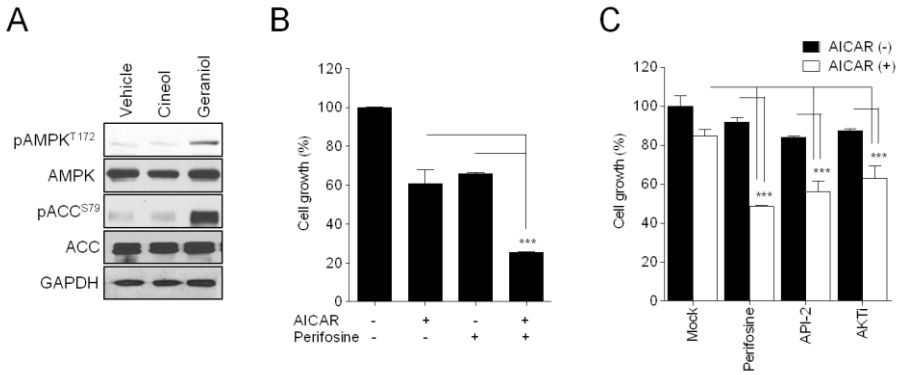


**Figure 13**. AMPK activation enhances the ability of AKT inhibitors to suppress tumor growth in PC-3 cells (A) The cells were treated with geraniol at the indicated concentrations for 4 h prior to Istern blot analyses. (B) The cells were treated with AICAR (1 mM) and/or perifosine (5 μM) for 72 h prior to MTT assays. Cell growth was expressed as a relative value compared to that of the untreated cells which was set to 100%. The data were expressed as the mean ± SEM (n=3). *** $P < 0.005$. (B) The cells were treated with AICAR (100 μM) and/or perifosine (2 μM), AKTi-1/2 (2 μM), or API-2 (5 μM) for 72 h prior to MTT assays. The data were expressed as the ± SEM (n=4). *** $P < 0.005$.

# Part 2

## 2.1 AKT inhibitors induce cell death

Androgen ablation therapy suppressed the progression of prostate cancer growth, but did not lead to complete regression of cancer growth. During cancer progression, the loss of function of PTEN cooperates in the development of CRPC cells via elevated AKT/mTOR pathway activity (Wang et al., 2003). Thus PTEN deficiency presents an efficient therapeutic target for treating CRPC cells. I employed AKT inhibitors in PC-3 cells to explore whether targeting of AKT induces suppression of CRPC cells growth. MTT assays showed that cell population gradually decreased in relation to concentrations of AKT inhibitors (Fig. 14A). AKT inhibitors induction of apoptosis was confirmed using caspase-3 activity assays. AKT inhibitors strongly increased caspase-3 activity in dose-dependent manners (Fig. 14C). I also examined analysis of apoptosis using flow cytometric assessment of annexin V–FITC–PI staining. In figure 14D, I observed the markedly higher apoptotic potential of AKT-inhibitors-treated PC-3 cells (Fig. 14D). In addition, I investigated whether perifosine/AKTi-1/2 inhibited AKT and activated caspase-3. Western blot analysis showed that AKT inhibitors inhibited AKT in a low dose and activated caspase-3 in a high dose (Fig. 14B). AKT inhibition was observed following treatment with AKT inhibitors for 12 h and was sustained thereafter (Fig. 14E). However, cleaved caspase-3 was

detected after 48 h. Although AKT was inhibited, I found that this did not lead to apoptosis directly.

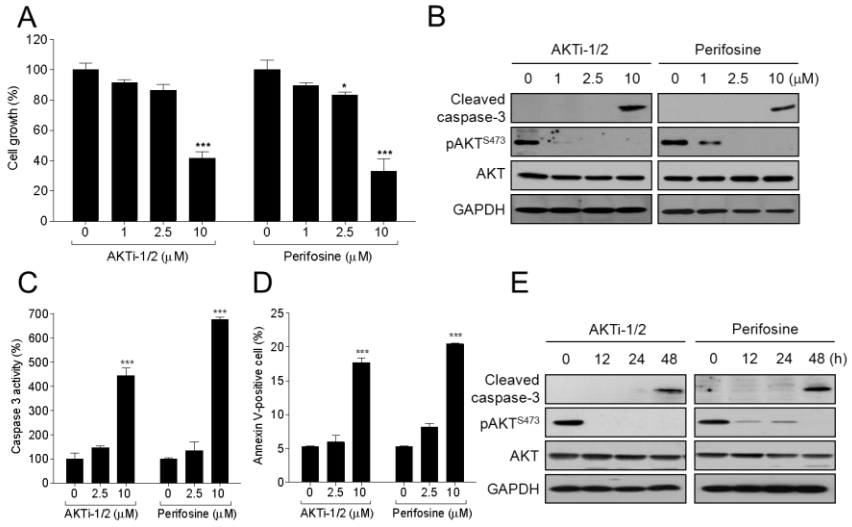


**Figure 14.** AKT inhibitor induces cell death in PC-3 cells. (A) The cells were treated with the Perifosine or AKTi-1/2 for 72 h prior to MTT assays. Cell growth was expressed as a relative absorbance value compared to that of vehicle-treated cells which was set to 100%. (B, E) Western blot analysis using the indicated antibodies. The crude extracts were prepared from the PC-3 cells treated with Perifosine or AKTi-1/2. GAPDH was used as a loading control. (C) Caspase-3 assays following treatment with Perifosine or AKTi-1/2 for 48 h. Caspase-3 activity from untreated cells is expressed as 100%. The figures show mean ± SEM (n=6). (D) The cells were treated with Perifosine or AKTi-1/2 for 48 h and then the cells were stained with annexin V-fluorescence isothiocyanate (FITC) and propidium iodide (PI) for flow cytometry analysis. The figures show mean ± SEM (n=4-6).

## 2.2 AKT knockdown does not induces apoptosis

Because AKT inhibitors inhibited cell growth and activity of AKT, I examined whether a specific knockdown of endogeneous AKT could induce significant inhibition of cell growth. MTT assays with knockdown AKT revealed unchanged growth of PC-3 cells (Fig. 15A), compared to AKT inhibitor induced cell death (Fig. 13A). Western blot analysis showed that AKT knockdown did not induce caspase-3 activity (Fig. 15B). These results raise the clue that to accelerate significant cell death, additional target responsible for the synthetic lethality could be needed. Thus, using network modeling by microarray analysis data, I found a subset of apoptosis related genes that may be formed a synthetic lethal interaction with AKT.

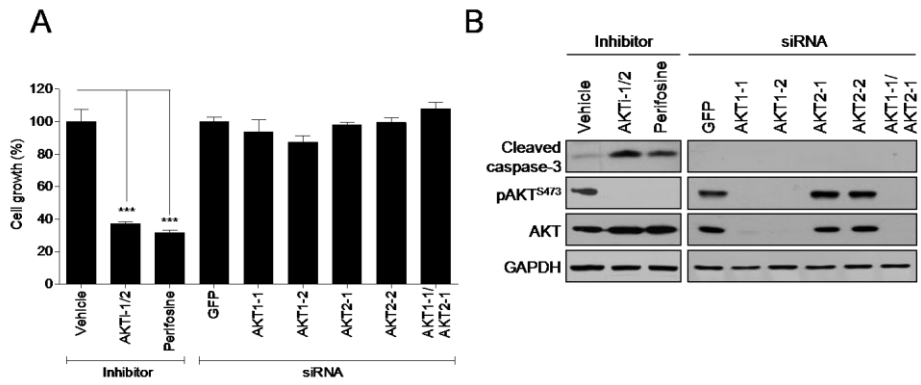


**Figure 15.** AKT knockdown does not induce cell death in PC-3 cells. (A) The cells were transfected with the indicated AKT siRNA for 72 h prior to MTT assays. Cell growth was expressed as a relative absorbance value compared to that of vehicle-treated cells which was set to 100%. (B) Western blot analysis using the indicated antibodies. The crude extracts were prepared from the PC-3 cells transfected with AKT siRNA for 72 h. GAPDH was used as a loading control.

### 2.3 E2F1 is a key hub that is closely located to AKT

By the analysis pipeline for network analysis, I first established a functional interaction network incorporating nearest neighbors of the seed genes: the common DEGs venn diagram of Perifosine and AKTi treated PC-3 cells (Fig. 16A), the heat map of common DEGs (Fig. 16B), and the heat map of K-means clustering gene signature (Fig. 16B). Figure 17 graphically represents the network model of PC-3 cells under the AKT inhibited conditions. Total 6,080 edges and 823 nodes were involved in the network model. Here, lozenge-shaped nodes denote the seed genes and circular-shaped nodes denote the nearest neighbor nodes. The color of nodes denotes gene expression profiles in AKT inhibited PC-3 cells. In the network model of PC-3 cells, AKT1 and E2F1 showed highly dense interactions with their neighbor nodes (neighbors of AKT1: 240, neighbors of E2F1: 512), comparing to other seed nodes (mean no. of neighbor: 31.1). GO-term enrichment analysis of K-means clustering result manifested all of seed nodes as candidates underlying cell death and cell cycle of PC-3 cells (Fig. 16D).

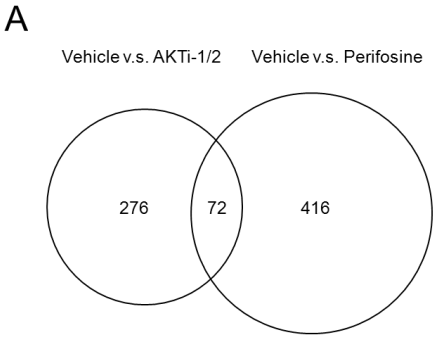


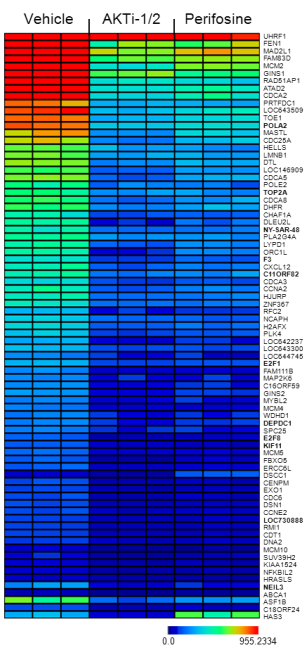


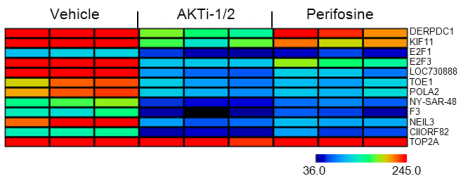


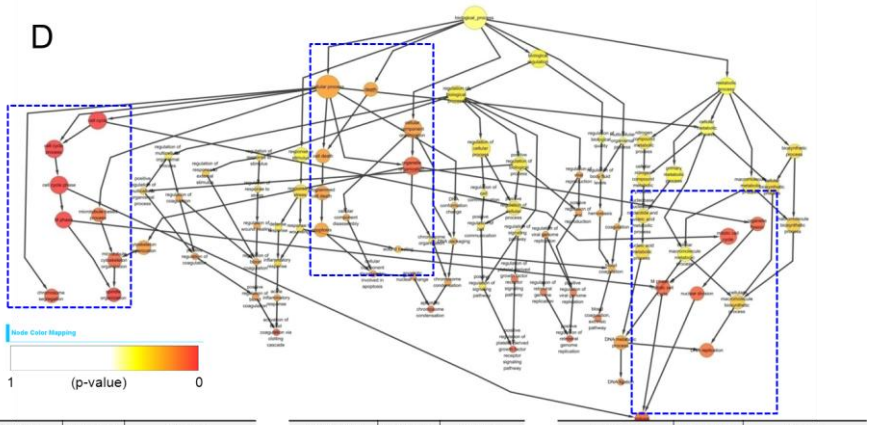


| GO term | p-value | Genes |
|---|---|---|
| Mitotic cell cycle | 0.00896 | E2F1, KIF11, NY-SAR-48 |
| Cell cycle phase | 0.00958 | E2F1, KIF11, NY-SAR-48 |
| Centrosome organization | 0.01512 | KIF11, NY-SAR-48 |
| Microtubule based process | 0.01707 | KIF11, NY-SAR-48 |
| Cell cycle process | 0.02151 | E2F1, KIF11, NY-SAR-48 |

| GO term | p-value | Genes |
|---|---|---|
| Apoptosis | 0.02290 | E2F1, F3, TOP2A |
| Programmed cell death | 0.02384 | E2F1, F3, TOP2A |
| Cell death | 0.02842 | E2F1, F3, TOP2A |
| Death | 0.02933 | E2F1, F3, TOP2A |

| GO term | p-value | Genes |
|---|---|---|
| DNA metabolic process | 0.02106 | NEIL3, POLA2, TOP2A |
| Nuclear division | 0.06491 | KIF11, NY-SAR-48 |
| Mitosis | 0.06491 | KIF11, NY-SAR-48 |
| M phase of mitotic cell cycle | 0.06741 | KIF11, NY-SAR-48 |
| Organelle fission | 0.06865 | KIF11, NY-SAR-48 |

**Figure 16.** Gene sets that are commonly regulated by AKT inhibitors. (A) Venn diagram of common DEGs (B) Heat map of common DEGs (C) Heat map of K-mean clustering gene signature. (D) GO analysis.

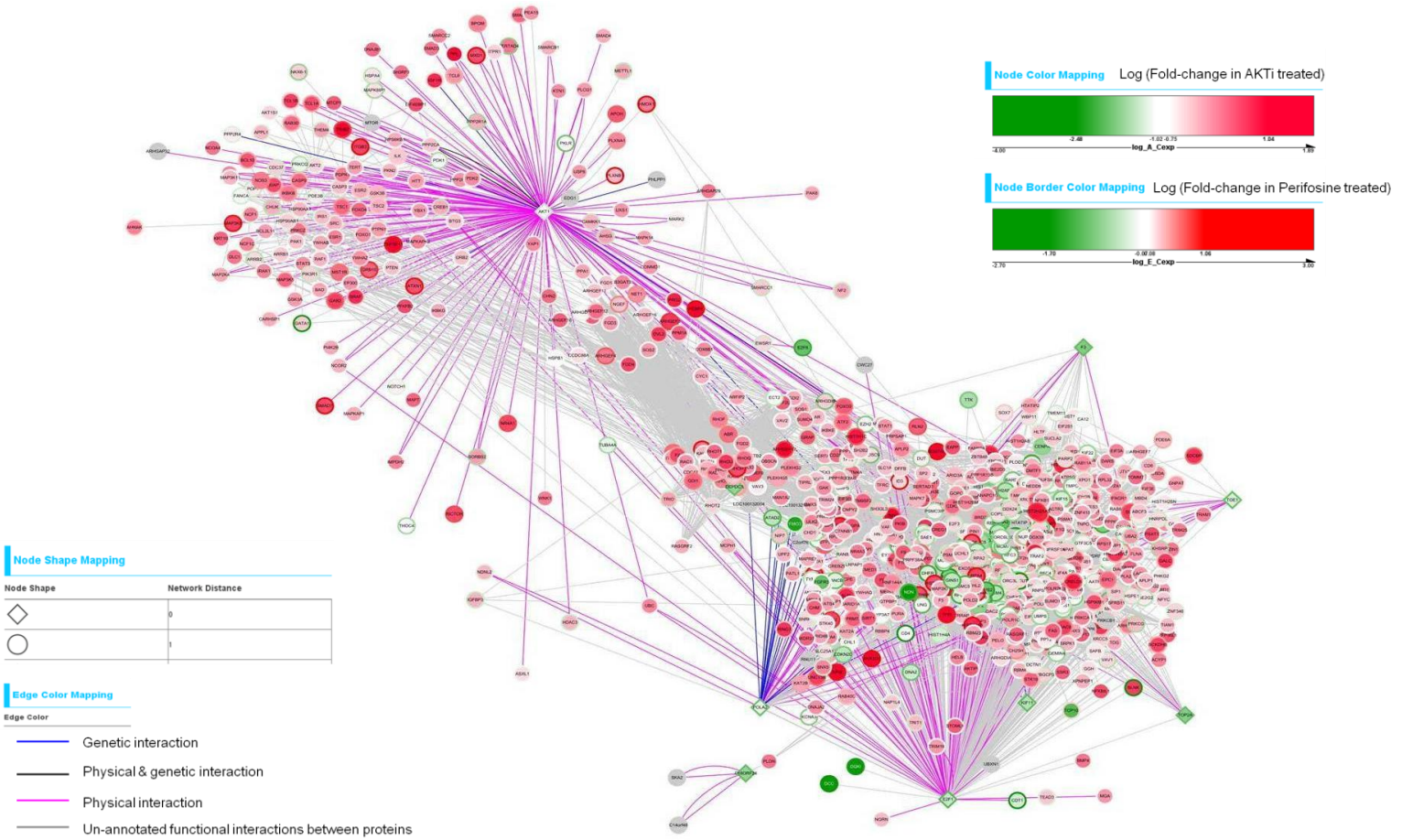
Node Color Mapping
Log (Fold-change in AKTi treated)
log_A_Cexp
Node Border Color Mapping
Log (Fold-change in Perifosine treated)
log_E_Cexp
Node Shape Mapping
Node Shape
Network Distance
Edge Color Mapping
Edge Color
Genetic interaction
Physical & genetic interaction
Physical interaction
Un-annotated functional interactions between proteins

**Figure 17.** The network model of PC-3 cells under the AKT inhibited conditions. Genes are represented by nodes and functional associations by edges, as indicated insets. Node color is indicated by fold-change in AKTi-1/2 treated. Node border is indicated by fold-change in Perifosine treated. Distance 0 of node shape is indicated by seed nodes, genes in cluster 7. Distance 1 of node shape is indicated by neighbor nodes.

### 2.4 AKT inhibitors down-regulate E2F1 expression

Consistent with the indirect evidence described above, E2F1, which was found to down-regulated in AKT inhibitors-treated with PC-3 cells, was tested. We performed RT-PCR for E2F1 gene in AKT inhibitors-treated PC-3 cells and observed the decreased transcriptional expression of E2F1 by AKT inhibitors treatment (Fig. 18A). In addition, western blot analysis showed that AKT inhibitors decreased the expression of E2F1 at 10 uM (Fig. 18B). To investigate whether E2F1 expression was regulated by transcriptional targets, I examined the luciferase activity assay using E2F reporter plasmid. As a result of it, I observed significant reduction of luciferase activity in a dose-dependent treatment of AKT inhibitors (data not shown).

Because AKT inhibitors induced down-regulation of E2F1 expression, I identified whether knockdown E2F1 has an effect on the viability of PC-3 cells. MTT assay showed a mild decrease of cell growth in siE2F1 transfected PC-3 cells. Moreover, Western blot analysis showed that E2F1 knockdown did not increase of caspase-3 activity (Fig. 18C). These results suggested that knockdown E2F1 did not cause cell death.

The expression of E2F2 also was down-regulalted by AKT inhibitors, but I verified E2F2 did not primarily involve in cellular pathway in PC-3 cells (Fig. 18D). These results showed that AKT inhibitors decrease the transcriptional expression of E2F1 in PC-3 cells.

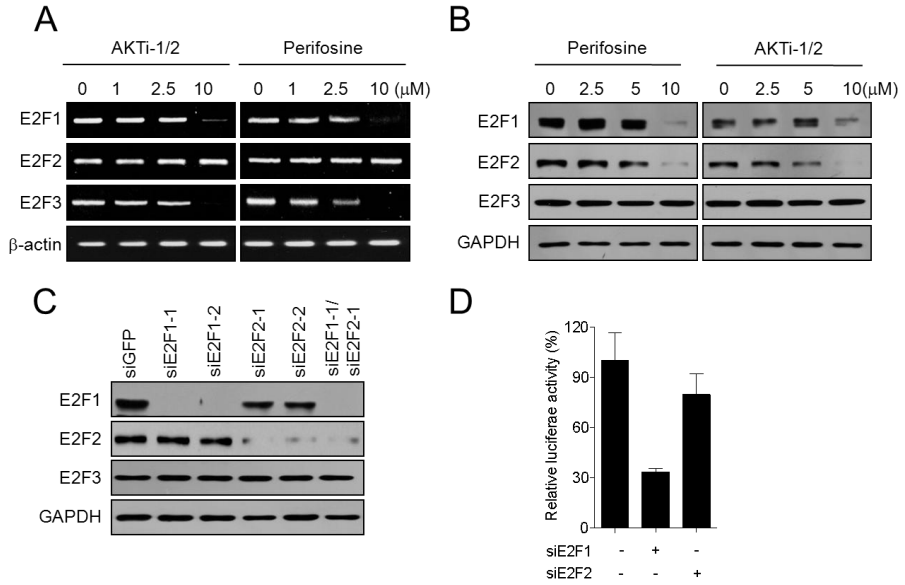


**Figure 18.** AKT inhibitors induce down-regulation of E2F1 in transcription level in PC-3 cells. (A) The cells were incubated with Perifosine or AKTi-1/2 for 24 h. The expression of E2F1 was detected by RT-PCR in PC-3 cells. β-actin was used as experimental control. (B) The cells were incubated with Perifosine or AKTi-1/2 for 24 h prior to Western blot analyses. Equal loading was ascertained based on GAPDH levels. (C) The cells were transfected with E2F1 siRNAs for 72 h prior to Western blot analyses. Equal loading was ascertained based on GAPDH levels. (D) The cells were transfected with E2F-luc reporter for 24 h and then treated with Perifosine or AKTi-1/2 for 24 h prior to Luciferase assays. Cell growth was expressed as a relative value compared to that of the untreated cells which was set to 100%. The data were expressed as the mean ± SEM (n=3). *** $P < 0.005$. (E)

The genetic and epigenetic changes that lead to cancer development are associated with aberrant gene expression including overexpression of genes compared with the normal state from which the cancers originated. PTEN is one of the most commonly lost tumor suppressor genes in human cancer including prostate cancer. Thus I analyzed the expression profile of the PTEN and E2F1 genes to compare transcript abundance in benign and metastatic stage using published data (GSE3325) (Fig. 19A and B). In the case of PTEN, a marked reduction of mRNA expression level was observed in metastatic stage. However, a marked increase of E2F1 mRNA was found in late stage. In these data suggested that E2F1 may be associated with the survival of the metastatic stage. In addition I established the heat map of E2F1 genetic signature in prostate cancer progression (Fig. 19C). These results showed that E2F1 and its signature significantly elevated in prostate cancer progression, but the gene signature was decreased in AKT inhibitor-treated PC-3 cells. E2F1 is up-regulated in CRPC cells as detected by both transcript and protein analyse, thus E2F1 may be important roles in survival of CRPC cells.

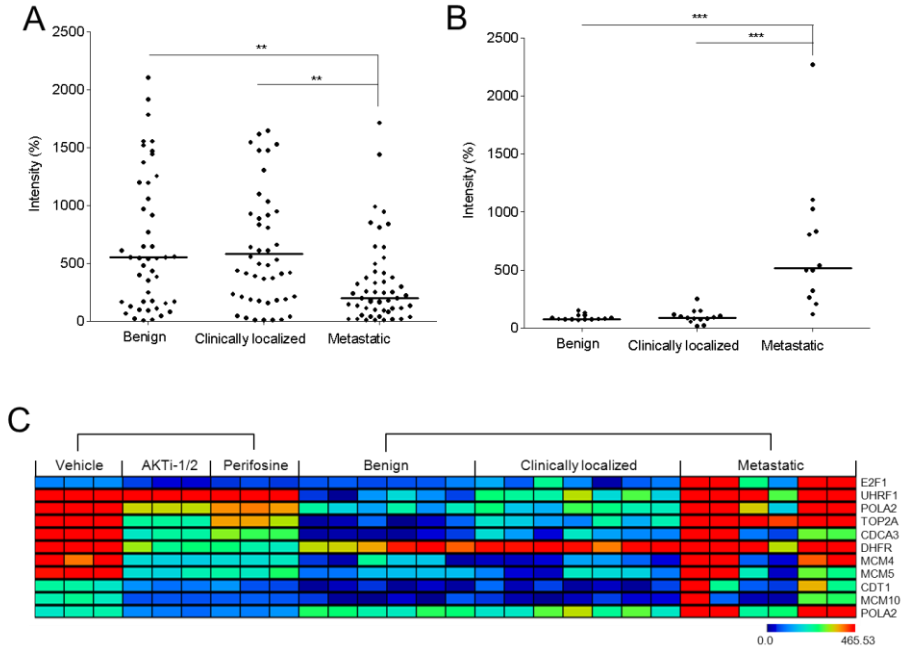


**Figure 19.** E2F1 and its gene signature in prostate cancer. (A) Intensity of PTEN/E2F1. (B) Heat map of E2F1 target genes.

## 2.5 The sub-network between AKT1 and E2F1 consists of receptor tyrosine kinase related genes

Our network model showed hub genes among seed nodes which interacted largest number of neighbor nodes (Figure 20). In figure 20, the sub-network of figure 17 was displayed, and nineteen nodes were identified as intermediate nodes between AKT1 and E2F1. These intermediate nodes, such as GAB2, STAT1, and CDKN1A, were potentially discussed as JAK-STAT, ErbB pathway related genes in previous studies, and GO enrichment analysis results also support these biological relevance with statistical evidences (*p-value* <0.05, Table 3). Therefore, our network modeling with DEG profiling, GO-term enrichment analysis and experimental results consistently pointed out E2F1 as a hub node which interacts with AKT1 in AKT1 inhibited PC-3 cells. In addition, the sub-network indicates that ErbB pathway may tightly relate to AKT and E2F1.

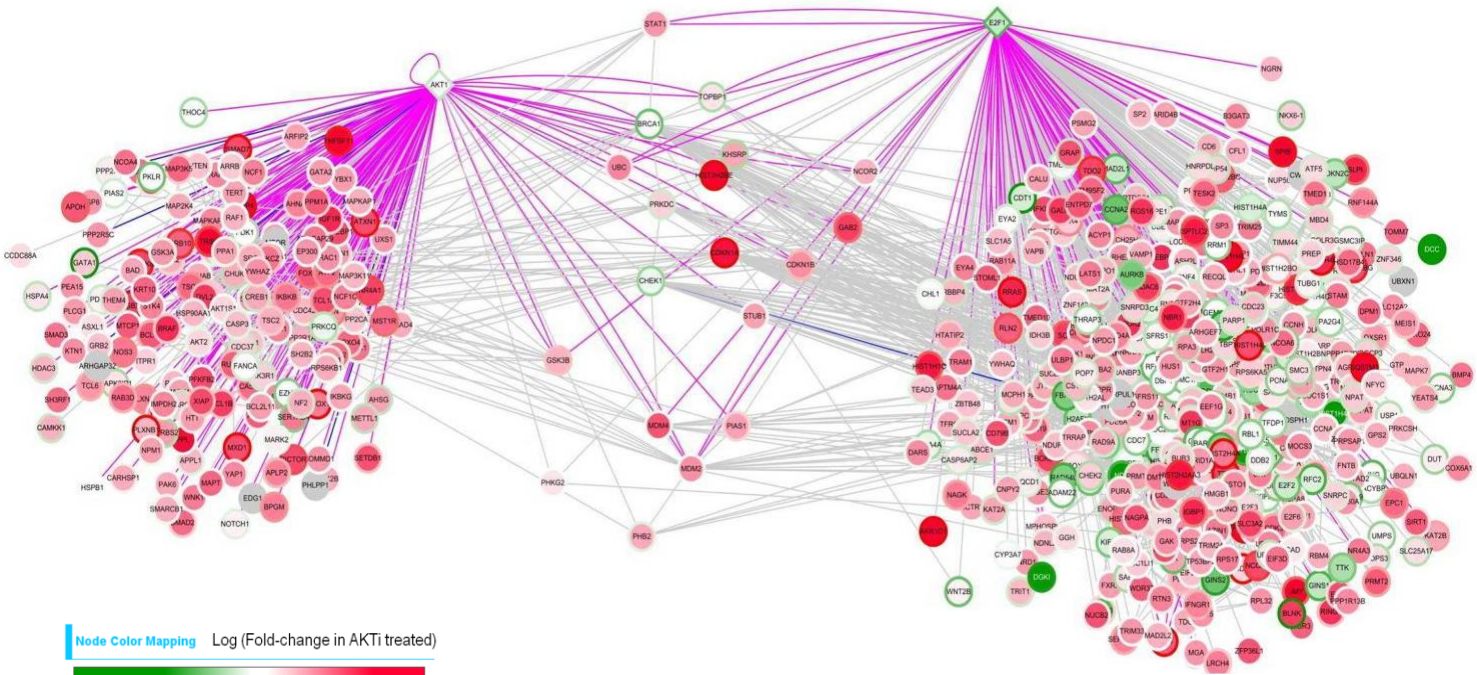
Node Color Mapping
Log (Fold-change in AKTi treated)
log_A_Cexp
Node Border Color Mapping
Log (Fold-change in Perifosine treated)
log_E_Cexp
Node Shape Mapping
Node Shape
Network Distance
Edge Color Mapping
Edge Color
Genetic interaction
Physical & genetic interaction
Physical interaction
Un-annotated functional interactions between proteins

**Figure 17.** The sub-network of figure 17, and nineteen nodes were identified as intermediate nodes between AKT1 and E2F1. Genes are represented by nodes and functional associations by edges, as indicated insets. Node color is indicated by fold-change in AKTi-1/2 treated. Node border is indicated by fold-change in Perifosine treated. Distance 0 of node shape is indicated by seed nodes, genes in cluster 7. Distance 1 of node shape is indicated by neighbor nodes.

## 2.6 Down-regulated E2F1 mediates decrease of RTK expression and activity

Our network analysis showed that the majority part of intermediate genes between AKT and E2F1 play critical roles on RTK signaling pathway. Recently, a number of studies reported that AKT inhibition relieves negative feedback loop of receptor tyrosine kinase activity and expression (Chandarlapaty et al., 2011; O'Reilly et al., 2006). But the relationship of E2F1 and RTK members has not clearly known yet. Therefore, to investigate whether RTK signaling pathway involve in the synthetic lethality of both genes, I performed dose-course analysis in AKT inhibitor-treated PC-3 cells. Western blot analysis showed that AKT inhibitors induced dephosphorylation of the AKT at 2.5 uM and decrease the protein expression levels of E2F1 at 10 uM (Fig. 20A ).

Akt inhibition caused a marked change in the phosphorylation and expression of RTK family members, but AKT inhibitors-mediated increase of RTK family activity was down-regulated at 10 uM (Fig. 20A). This dose also caused a decrease of E2F1 expression. To confirm AKT inhibition relieves the negative feedback network, as well as down-regulation of E2F1 expression induces decrease of RTK activity and expression, I performed Western blot analysis with knockdown of AKT and/or E2F1. I found that AKT knockdown induced increase the activity of RTK members and knockdown of both AKT and E2F1 induced inactivation of RTK members, resulting in significant cell

death (Fig. 20B). Thus I could draw a conclusion that down-regulation of E2F1 expression effects on the activity and expression of RTK family members.

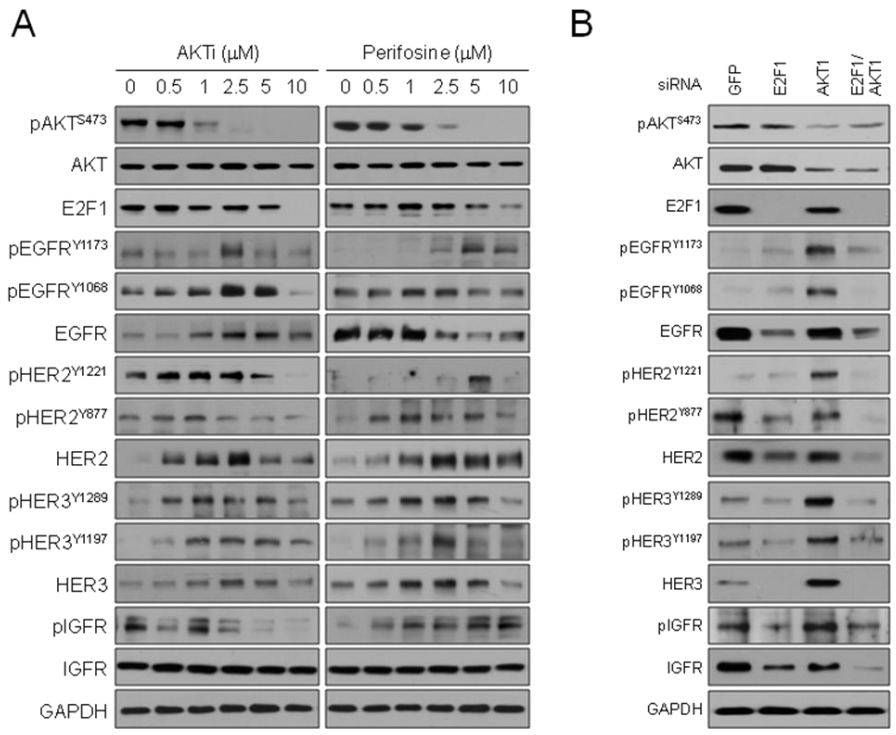


**Figure 20.** Inhibition of E2F1 down-regulates activated RTK family induced by AKT inhibition. (A) The cells were treated with Perifosine or AKTi 1/2 at the indicated concentrations for 24 h prior to Western blot analysis. (B) The cells were transfected with siAKT1 or/and siE2F1 at the indicated concentrations for 72 h prior to Western blot analyses.

## 2.7 Combined suppression of AKT and E2F1 expression induces apoptosis

Synthetic lethality is a novel therapeutic paradigm for the development of cancer-specific targeting approaches (Iglehart and Silver, 2009; Kaelin, 2005). The principle of synthetic lethality is base on the loss of function of two genes, resulting in significant increase of cell death (Kaelin, 2005). For achieving a deeper understanding of genetic interaction, I used network modeling in above study to identify systematically critical gene involving on cell death. Thus I obtained down-regulated E2F1 gene in AKT inhibitors-treated PC-3 cells. To identify synthetic lethality of AKT and E2F1, I experimented whether knockdown of both genes leads to significant cell death. MTT assay showed that simultaneous knockdown both of genes induced significant decrease of cell growth, while knockdown of either gene alone is compatible with viability in PC-3 cells (Fig. 21A up).

I then performed western blotting to evaluate increase of cell death. As a result of it, knockdown of both genes increases caspase activity (Fig. 21A botton). In addition, knockdown of AKT and/or E2F1 induced the change of Bcl-2 family expression level, leading to cell death. E2F1 knockdown induced increase the expression of anti-apoptotic protein, Bcl-2 (Fig. 21A botton). AKT knockdown induced increase activity and the expression of pro-apoptotic protein, Bax, and decrease the Bcl-2 expression level (Fig. 21A botton). These results suggest that knockdown of both genes, E2F1 and AKT,

induced significant cell death via regulating Bcl-2 family.

Because AKT inhibition relieves negative feedback network, expression levels of RTK pathway is increased. But down-regulated E2F1 suppresses AKT-induced RTK expression. Therefore E2F1 knockdown induced inactivation of RTK members. I used siE2F1 to test whether blocking RTK activity enhances anti-cancer effect of AKT inhibitors. MTT assay showed that individual treatment of low dose AKT inhibitors did not induce decrease of cell growth, but treatment of AKT inhibitor with E2F1 knockdown caused significant cell suppressions in PC-3 cells (Fig. 21B up).

Next I performed western blotting to evaluate increase of cell death. As a result of it, treatment of AKT inhibitor with E2F1 knockdown increases caspase activity (Fig. 21B botton). In addition, treatment of AKT and/or E2F1 knockdown induced the change of Bcl-2 family expression level, leading to cell death. E2F1 knockdown induced increase the expression of anti-apoptotic protein, Bcl-2 (Fig. 21B botton). Treatment of AKT inhibitors induced increase activity and the expression of pro-apoptotic protein, Bax, and decrease the Bcl-2 expression level (Fig. 21B botton). These results suggest that E2F1 inhibition is sufficient to prevent relief of negative feedback loop induced by AKT inhibitors. Thus I found that blocking RTK pathway with E2F1 inhibition sensitizes cells to AKT inhibitors and induces significant prostate cancer cells suppression.

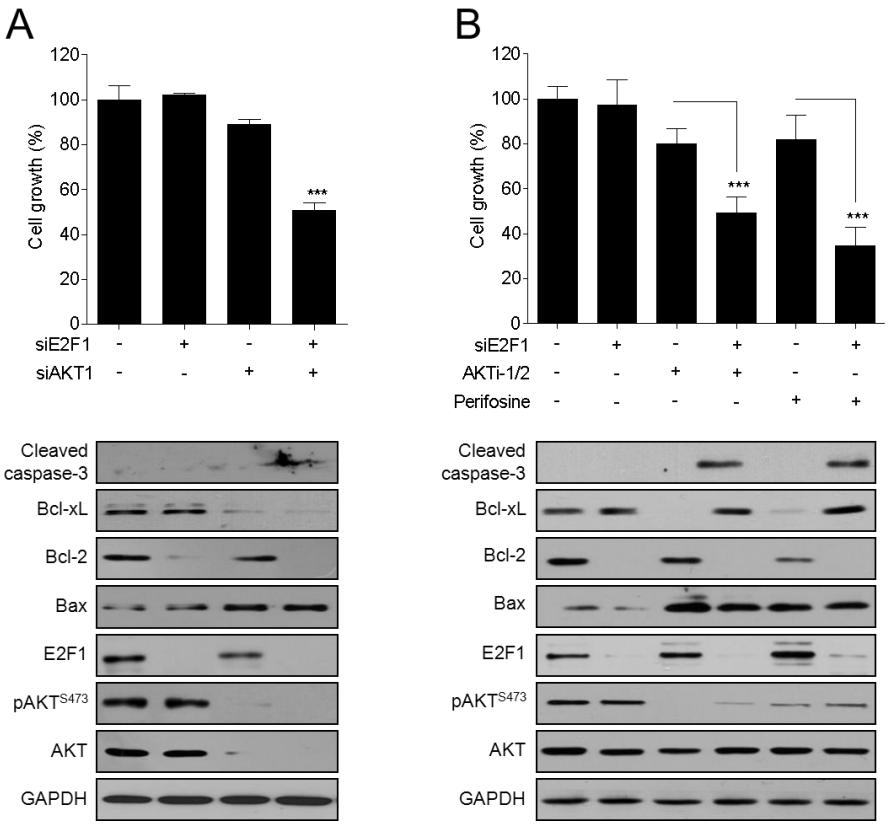
A
Cell growth (%)
120
100
80
60
40
20
0
***
siE2F1 - + - +
siAKT1 - - + +
B
Cell growth (%)
120
100
80
60
40
20
0
***
***
siE2F1 - + - + - +
AKTi-1/2 - - + + - -
Perifosine - - - - + +
Cleaved caspase-3
Bcl-xL
Bcl-2
Bax
E2F1
pAKTS473
AKT
GAPDH
Cleaved caspase-3
Bcl-xL
Bcl-2
Bax
E2F1
pAKTS473
AKT
GAPDH

**Figure 21.** Combined inhibition of AKT and E2F1 expression induces apoptosis. (A up) The cells were transfected with siAKT1 or/and siE2F1 for 72 h prior to MTT assays. Cell growth was expressed as a relative value compared to that of the untreated cells which was set to 100%. The data were expressed as the mean ± SEM (n=3). *** $P < 0.005$. (A botton) The cells were transfected with siAKT1 or/and siE2F1 for 72 h prior to Western blot analyses. (B up) The cells were transfected with siE2F1 for 48 h and then incubated with AKTi1/2 (2.5 uM) or Perifosine (2.5 uM) for 48 h prior to MTT assays. Cell growth was expressed as a relative value compared to that of the untreated cells which was set to 100%. The data were expressed as the mean ± SEM (n=3). *** $P < 0.005$. (B botton) The cells were transfected with siE2F1 for 48 h and then incubated with AKTi1/2 or Perifosine for 48 h prior to Western blot analyses.

# IV. Discussion

Androgen exerts its actions through androgen receptor (AR), a crucial effector molecule of prostate cancer development and progression (Heinlein and Chang, 2004). Androgen ablation initially suppresses tumor growth via triggering cell death in prostate cancer cells (Denmeade et al., 1996; Westin et al., 1995). However, it acts as a selection pressure to allow cancer cells to evolve evading mechanisms that restore AR activity (Debes and Tindall, 2004; Feldman and Feldman, 2001). Therefore, prostate cancer cells escape from cell death occurring under androgen-ablated conditions and eventually CRPC emerges, resulting in clinical relapse (Harris et al., 2009). Indeed, prostate cancer cells accumulate the mutations that lead to the defects in cell cycle checkpoints and eventually cell cycle misregulation (Agus et al., 1999; Karan et al., 2002; LaTulippe et al., 2002) and anti-apoptotic proteins are up-regulated in high grade or relapsed prostate cancer (Catz and Johnson, 2003; Chaudhary et al., 1999; McDonnell et al., 1992). In addition PTEN loss has been represented as a strong cause of resistance in CRPC (Hollander et al., 2011; Jiao et al., 2007; Shen and Abate-Shen, 2007). PTEN loss may play critical roles in a cell autonomous manner to enhance AR-independent CRPC progression. Together with these observations, our data highlight the importance of the strategy for targeting dysregulated cellular pathways to promote the bypass mechanisms of CRPC acquired under androgen-depleted conditions.

In this study, I described two main findings. In part 1, I employed geraniol as a lead compound for future development of anti-tumor drugs and chemical probe for understanding of CRPC cellular mechanism and identifying new therapeutic targets. Thus, first I found that geraniol suppresses PC-3 cell growth in culture and xenograft models and the anticancer activity of geraniol is attributable to cell cycle arrest and/or apoptosis. In addition, geraniol increases the sensitivity of PC-3 cells to chemotherapeutic agents. Second, I demonstrated that geraniol induced apoptosis and autophagy, which occurred independently of each other, and combined inhibition both of cell death types restored cell growth in geraniol-treated cells. In addition, geraniol inhibited AKT and activated AMPK signaling and the combined modulation of AKT and AMPK is more effective than either alone in prostate cancer therapy. Together with these evidences, I could raise the hypothesis that targeting of PTEN-induced activated AKT-mTOR pathway may promote profound cell killing. Thus, in part 2, I used AKT inhibitors to investigate whether inhibition of AKT have an effect on CRPC cells viability. In this study, I found that AKT inhibition induces the increase activity and expression of RTK, but suppression of E2F1 promotes down-regulation of RTK activity and expression. Consequently, combined inhibition of AKT-mTOR and E2F1 causes significant regression of CRPC cells growth. Our results indicate that targeting both of genes is applicable for future development of anticancer drugs. Furthermore our findings provide a

basis for future investigations that are aimed at elucidating the role of apoptosis and autophagy in prostate cancer therapy.

CRPC is notoriously resistant to available chemotherapeutic regimens and its prognosis is highly poor (Chen et al., 2004; Nelson et al., 2003). Previously, flavopiridol (a small molecule CDK inhibitor) and docetaxel have shown anti-tumor effects against several types of cancers in clinical setting (Fornier et al., 2007). Flavopiridol induces cell cycle arrest and apoptosis in cancer cells, suggesting that the therapeutic strategy cotargeting cell cycle and apoptosis can be useful to increase chemosensitivity (Bible and Kaufmann, 1997; Matranga and Shapiro, 2002). Here I showed that geraniol can be a promising chemosensitizer through cotargeting cell cycle and apoptosis. Tumor graft experiments demonstrated that geraniol at sub-toxic dose increases the sensitivity of PC-3 cells to docetaxel at sub-toxic dose. These results indicate that geraniol may circumvent the clinical problem of chemoresistance of CRPC.

A strategy to restore the ability to induce cell death is needed to improve therapy for castration-resistant prostate cancer. However, cell death is a complex phenomenon that is independently or interactively regulated by multiple cellular and molecular mechanisms (Eisenberg-Lerner et al., 2009; Lockshin and Zakeri, 2004). Therefore I showed that combined inhibition of apoptosis and autophagy markedly restored cell growth, compared to

inhibition of either process alone. These results suggest that these processes synergistically interact with each other to induce cell death. Our time-course analysis showed that autophagy preceded apoptosis in geraniol-treated cells. However, the results also suggest that apoptosis and autophagy are independently processes. Taken together, our results suggest that although these processes do not affect each other, the cooperation of apoptosis and autophagy after their induction is crucial to elicit cell death. Further studies using geraniol as a chemical probe may assist in understanding the phenotypic complexity of the relationship between apoptosis and autophagy at a molecular level.

Apoptosis and autophagy share common molecular regulators and pathways (Fimia and Piacentini, 2010; Maiuri et al., 2007). However, the phenotypic outcome of the interaction between these processes is extremely complex because apoptosis and autophagy exhibit synergistic or antagonistic effects on each other in cell death (Eisenberg-Lerner et al., 2009; Thorburn, 2008). The mechanisms that generate this phenotypic complexity have not been well characterized. Furthermore, autophagy that is induced by clinically available anticancer agents has been reported to protect cancer cells from apoptotic cell death depending on the cell type and/or context (Chen et al., 2010; Dalby et al., 2010). Therefore, understanding the crosstalk between apoptosis and autophagy may be crucial for the development of therapeutic strategies to improve the efficacy of anticancer agents.

AKT inhibition and AMPK activation commonly resulted in mTOR inhibition (Inoki et al., 2003). Our results showed that the combined effect of AKT inhibition and AMPK activation is more potent in suppressing prostate cancer growth than either alone. Because mTOR inhibition (*e.g*. rapamycin treatment) induces growth arrest rather than cell death (Hidalgo and Rowinsky, 2000; Huang and Houghton, 2003), mTOR inhibition seems to be one of the molecular mechanisms underlying the combined effect of AKT inhibition and AMPK activation. AKT or mTOR inhibition is not clinically successful in prostate cancer treatment (Engelman, 2009). Therefore, our findings provide insight into future investigations that are aimed at developing the anticancer co-targeting strategies for prostate cancer therapy.

AKT/mTOR pathway has been shown to promote prostate tumorigenicity and androgen refractory development. Because AKT/mTOR pathway is a downstream effector of RTK family, activated AKT/mTOR pathway lead to inhibition of RTK family via negative feedback network (O'Reilly et al., 2006). Although the mechanism is not completely understood, increasing evidences suggest that AKT/mTOR inhibition induces increase of activity and expression of RTK family (Chandarlapaty et al., 2011; O'Reilly et al., 2006). Therefore I employed optimal dose of AKT inhibitors, AKTi-1/2 or Perifosine, to test whether inhibition of AKT does not induce cell death in CRPC. In this study, optimal dose of AKT inhibitors that dephosphorylates

AKT did not induce significant cell death. These results are consistent with the idea that AKT knockdown does not induce cell death, because inhibition of AKT causes only autophagy but not apoptosis (Degtyarev et al., 2008). These finding suggest that inhibition of AKT doesn′t induce suppression of CRPC cells, therefore to increase therapeutic efficacy I need to investigate critical molecule promoting apoptosis.

Recently, systematical researches for mutated oncogenes that can be targeted by anti-cancer drugs serve highthrough-put database of cancer genetics for successful therapeutic approach. Thus I used network analysis based on integration of datasets from various species to infer a novel molecule having synthetic lethal relationship with AKT. Our genetic analysis supports that AKT inhibitors affect apoptosis-linked gene sets. Particularly, down-regulated E2F1 that is a critical hub in network model functions as excellent target for anti-cancer treatment strategies because of the following reasons: E2F1 is overexpressed in high–grade cancer (Davis et al., 2006; Nevins, 2001; Zacharatos et al., 2004); Although E2F1 functions as a double-edges sword for cancer cells, the elevated level of E2F1 primarily involves the development of p53 mutated cancer cells. Because CDK inhibitor, such as $p16^{INK4a}$, regulating of the Rb-E2F1 pathway is mutated in CRPC cells, E2F1 is accumulated in CRPC cells (Nevins, 2001); In our interactome network models on the basis of a combination of different genetic interactions, E2F1

has more connected nodes and more edges. Therefore I raise the possibility that synthetic lethal targeting of E2F1 and AKT provide a framework for identifying effective anti-cancer strategy.

In this study, I found that inhibition of both AKT and E2F1 induced significant suppression of CRPC cells. Although AKT knockdown did not affect cell viability, knockdown both of genes suppressed cell growth due to down-regulating activity and expression of RTK by E2F1. It has been reported that inhibition of E2F1-induced apoptosis associated with AKT pathway (Chaussepied and Ginsberg, 2004; Ladu et al., 2008). Grb-associated binder 2, GAB2, is demonstrated as a target gene of E2F1, which is responsible for the activation of AKT by E2F1 (Chaussepied and Ginsberg, 2004). But $GAB2^{-/-}$ did not change AKT activity in RTK overexpressed cancer (Ke et al., 2007). Thus the mechanism of AKT regulated control of E2F1 is not completely understood. Moreover, because individual knockdown of a single E2F1 or AKT had no effect on the expression levels of the other protein, AKT or E2F1, I demonstrated that AKT and E2F1 are independently regulated by multiple cellular pathways.

The robustness and redundancy of biological network of cancer cells suggest that single target drug discovery has a limitation for solving clinical challenges like chemoresistance. Thus, multitarget drug discovery or polypharmacology is emerging as a promising anticancer approach (Hopkins,

2008). In part 1, I show that geraniol is a multitarget agent affecting the expression level of various cell cycle- and apoptosis/autophagy-related proteins. Accordingly, geraniol can be used as a valuable chemical moiety for fragment-based drug discovery. In addition, the action mechanisms of geraniol provide insight into the development of novel therapeutic strategies. Together with these clues, I investigate that combined inhibition of AKT and feedback loop of RTK could have enhanced anti-tumor activity. Network analysis suggests that E2F1 is a critical apoptosis-related hub protein to induce synthetic lethality phenotype with AKT. Thereby I found that optimal dose of AKT inhibitors induce CRPC cells suppression when combined with knockdown of E2F1, because suppression of E2F1 prevents induction of RTKs phosphorylayion. Whether effective inhibition of both AKT and E2F1 pathway will have an effective therapeutic strategy and it will have to be evaluated in clinical trials.

# V. References

Agus, D.B., Cordon-Cardo, C., Fox, W., Drobnjak, M., Koff, A., Golde, D.W., and Scher, H.I. (1999). Prostate cancer cell cycle regulators: response to androgen withdrawal and development of androgen independence. J Natl Cancer Inst *91*, 1869-1876.

Behrendt, H.J., Germann, T., Gillen, C., Hatt, H., and Jostock, R. (2004). Characterization of the mouse cold-menthol receptor TRPM8 and vanilloid receptor type-1 VR1 using a fluorometric imaging plate reader (FLIPR) assay. Br J Pharmacol *141*, 737-745.

Bible, K.C., and Kaufmann, S.H. (1997). Cytotoxic synergy between flavopiridol (NSC 649890, L86-8275) and various antineoplastic agents: the importance of sequence of administration. Cancer Res *57*, 3375-3380.

Carnesecchi, S., Schneider, Y., Ceraline, J., Duranton, B., Gosse, F., Seiler, N., and Raul, F. (2001). Geraniol, a component of plant essential oils, inhibits growth and polyamine biosynthesis in human colon cancer cells. J Pharmacol Exp Ther *298*, 197-200.

Carver, B.S., Chapinski, C., Wongvipat, J., Hieronymus, H., Chen, Y., Chandarlapaty, S., Arora, V.K., Le, C., Koutcher, J., Scher, H., *et al.* (2011). Reciprocal feedback regulation of PI3K and androgen receptor signaling in PTEN-deficient prostate cancer. Cancer Cell *19*, 575-586.

Catz, S.D., and Johnson, J.L. (2003). BCL-2 in prostate cancer: a minireview. Apoptosis *8*, 29-37.

Chandarlapaty, S., Sawai, A., Scaltriti, M., Rodrik-Outmezguine, V., Grbovic-Huezo, O., Serra, V., Majumder, P.K., Baselga, J., and Rosen, N. (2011). AKT inhibition relieves feedback suppression of receptor tyrosine kinase expression and activity. Cancer Cell *19*, 58-71.

Chaudhary, K.S., Abel, P.D., and Lalani, E.N. (1999). Role of the Bcl-2 gene family in prostate cancer progression and its implications for therapeutic intervention. Environ Health Perspect *107 Suppl 1*, 49-57.

Chaussepied, M., and Ginsberg, D. (2004). Transcriptional regulation of AKT activation by E2F. Mol Cell *16*, 831-837.

Chen, C.D., Welsbie, D.S., Tran, C., Baek, S.H., Chen, R., Vessella, R., Rosenfeld, M.G., and Sawyers, C.L. (2004). Molecular determinants of resistance to antiandrogen therapy. Nat Med *10*, 33-39.

Chen, M., Pratt, C.P., Zeeman, M.E., Schultz, N., Taylor, B.S., O'Neill, A., Castillo-Martin, M., Nowak, D.G., Naguib, A., Grace, D.M., *et al.* (2011). Identification of PHLPP1 as a tumor suppressor reveals the role of feedback activation in PTEN-mutant prostate cancer progression. Cancer Cell *20*, 173-186.

Chen, M.L., Xu, P.Z., Peng, X.D., Chen, W.S., Guzman, G., Yang, X., Di Cristofano, A., Pandolfi, P.P., and Hay, N. (2006). The deficiency of Akt1 is sufficient to suppress tumor development in Pten+/- mice. Genes Dev *20*, 1569-1574.

Chen, S., Rehman, S.K., Zhang, W., Wen, A., Yao, L., and Zhang, J. (2010). Autophagy is a therapeutic target in anticancer drug resistance. Biochim

Biophys Acta *1806*, 220-229.

Codogno, P., and Meijer, A.J. (2005). Autophagy and signaling: their role in cell survival and cell death. Cell Death Differ *12 Suppl 2*, 1509-1518.

Dalby, K.N., Tekedereli, I., Lopez-Berestein, G., and Ozpolat, B. (2010). Targeting the prodeath and prosurvival functions of autophagy as novel therapeutic strategies in cancer. Autophagy *6*, 322-329.

Danial, N.N., and Korsmeyer, S.J. (2004). Cell death: critical control points. Cell *116*, 205-219.

Davis, J.N., Wojno, K.J., Daignault, S., Hofer, M.D., Kuefer, R., Rubin, M.A., and Day, M.L. (2006). Elevated E2F1 inhibits transcription of the androgen receptor in metastatic hormone-resistant prostate cancer. Cancer Res *66*, 11897-11906.

Debes, J.D., and Tindall, D.J. (2004). Mechanisms of androgen-refractory prostate cancer. N Engl J Med *351*, 1488-1490.

Degtyarev, M., De Maziere, A., Orr, C., Lin, J., Lee, B.B., Tien, J.Y., Prior, W.W., van Dijk, S., Wu, H., Gray, D.C., *et al.* (2008). Akt inhibition promotes autophagy and sensitizes PTEN-null tumors to lysosomotropic agents. J Cell Biol *183*, 101-116.

Denmeade, S.R., Lin, X.S., and Isaacs, J.T. (1996). Role of programmed (apoptotic) cell death during the progression and therapy for prostate cancer. Prostate *28*, 251-265.

Eisenberg-Lerner, A., Bialik, S., Simon, H.U., and Kimchi, A. (2009). Life and death partners: apoptosis, autophagy and the cross-talk between them.

Cell Death Differ *16*, 966-975.

Ellis, L.M., and Hicklin, D.J. (2009). Resistance to Targeted Therapies: Refining Anticancer Therapy in the Era of Molecular Oncology. Clin Cancer Res *15*, 7471-7478.

Engelman, J.A. (2009). Targeting PI3K signalling in cancer: opportunities, challenges and limitations. Nat Rev Cancer *9*, 550-562.

Feldman, B.J., and Feldman, D. (2001). The development of androgen-independent prostate cancer. Nat Rev Cancer *1*, 34-45.

Fimia, G.M., and Piacentini, M. (2010). Regulation of autophagy in mammals and its interplay with apoptosis. Cell Mol Life Sci *67*, 1581-1588.

Fornier, M.N., Rathkopf, D., Shah, M., Patil, S., O'Reilly, E., Tse, A.N., Hudis, C., Lefkowitz, R., Kelsen, D.P., and Schwartz, G.K. (2007). Phase I dose-finding study of weekly docetaxel followed by flavopiridol for patients with advanced solid tumors. Clin Cancer Res *13*, 5841-5846.

Ganjewala, D., and Luthra, R. Essential oil biosynthesis and regulation in the genus Cymbopogon. Nat Prod Commun *5*, 163-172.

Gao, H., Ouyang, X., Banach-Petrosky, W.A., Shen, M.M., and Abate-Shen, C. (2006). Emergence of androgen independence at early stages of prostate cancer progression in Nkx3.1; Pten mice. Cancer Res *66*, 7929-7933.

Gozuacik, D., and Kimchi, A. (2004). Autophagy as a cell death and tumor suppressor mechanism. Oncogene *23*, 2891-2906.

Grant, S., and Roberts, J.D. (2003). The use of cyclin-dependent kinase inhibitors alone or in combination with established cytotoxic drugs in cancer

chemotherapy. Drug Resist Updat *6*, 15-26.

Hanahan, D., and Weinberg, R.A. (2000). The hallmarks of cancer. Cell *100*, 57-70.

Harris, W.P., Mostaghel, E.A., Nelson, P.S., and Montgomery, B. (2009). Androgen deprivation therapy: progress in understanding mechanisms of resistance and optimizing androgen depletion. Nat Clin Pract Urol *6*, 76-85.

Heinlein, C.A., and Chang, C. (2004). Androgen receptor in prostate cancer. Endocr Rev *25*, 276-308.

Hidalgo, M., and Rowinsky, E.K. (2000). The rapamycin-sensitive signal transduction pathway as a target for cancer therapy. Oncogene *19*, 6680-6686.

Hochegger, H., Takeda, S., and Hunt, T. (2008). Cyclin-dependent kinases and cell-cycle transitions: does one fit all? Nat Rev Mol Cell Biol *9*, 910-916.

Hollander, M.C., Blumenthal, G.M., and Dennis, P.A. (2011). PTEN loss in the continuum of common cancers, rare syndromes and mouse models. Nat Rev Cancer *11*, 289-301.

Hopkins, A.L. (2008). Network pharmacology: the next paradigm in drug discovery. Nat Chem Biol *4*, 682-690.

Huang, S., and Houghton, P.J. (2003). Targeting mTOR signaling for cancer therapy. Curr Opin Pharmacol *3*, 371-377.

Iglehart, J.D., and Silver, D.P. (2009). Synthetic lethality--a new direction in cancer-drug development. N Engl J Med *361*, 189-191.

Inoki, K., Zhu, T., and Guan, K.L. (2003). TSC2 mediates cellular energy response to control cell growth and survival. Cell *115*, 577-590.

Jemal, A., Bray, F., Center, M.M., Ferlay, J., Ward, E., and Forman, D. Global cancer statistics. CA Cancer J Clin.

Jiao, J., Wang, S., Qiao, R., Vivanco, I., Watson, P.A., Sawyers, C.L., and Wu, H. (2007). Murine cell lines derived from Pten null prostate cancer show the critical role of PTEN in hormone refractory prostate cancer development. Cancer Res *67*, 6083-6091.

Kaelin, W.G., Jr. (2005). The concept of synthetic lethality in the context of anticancer therapy. Nat Rev Cancer *5*, 689-698.

Karan, D., Kelly, D.L., Rizzino, A., Lin, M.F., and Batra, S.K. (2002). Expression profile of differentially-regulated genes during progression of androgen-independent growth in human prostate cancer cells. Carcinogenesis *23*, 967-975.

Ke, Y., Wu, D., Princen, F., Nguyen, T., Pang, Y., Lesperance, J., Muller, W.J., Oshima, R.G., and Feng, G.S. (2007). Role of Gab2 in mammary tumorigenesis and metastasis. Oncogene *26*, 4951-4960.

Kim, S.H., Bae, H.C., Park, E.J., Lee, C.R., Kim, B.J., Lee, S., Park, H.H., Kim, S.J., So, I., Kim, T.W., *et al.* (2011). Geraniol inhibits prostate cancer growth by targeting cell cycle and apoptosis pathways. Biochem Biophys Res Commun *407*, 129-134.

Kim, S.H., Nam, J.H., Park, E.J., Kim, B.J., Kim, S.J., So, I., and Jeon, J.H. (2009). Menthol regulates TRPM8-independent processes in PC-3 prostate cancer cells. Biochim Biophys Acta *1792*, 33-38.

Kreisberg, J.I., Malik, S.N., Prihoda, T.J., Bedolla, R.G., Troyer, D.A.,

Kreisberg, S., and Ghosh, P.M. (2004). Phosphorylation of Akt (Ser473) is an excellent predictor of poor clinical outcome in prostate cancer. Cancer Res *64*, 5232-5236.

Ladu, S., Calvisi, D.F., Conner, E.A., Farina, M., Factor, V.M., and Thorgeirsson, S.S. (2008). E2F1 inhibits c-Myc-driven apoptosis via PIK3CA/Akt/mTOR and COX-2 in a mouse model of human liver cancer. Gastroenterology *135*, 1322-1332.

Lapczynski, A., Bhatia, S.P., Foxenberg, R.J., Letizia, C.S., and Api, A.M. (2008). Fragrance material review on geraniol. Food Chem Toxicol *46 Suppl 11*, S160-170.

LaTulippe, E., Satagopan, J., Smith, A., Scher, H., Scardino, P., Reuter, V., and Gerald, W.L. (2002). Comprehensive gene expression analysis of prostate cancer reveals distinct transcriptional programs associated with metastatic disease. Cancer Res *62*, 4499-4506.

Lee, J.T., Lehmann, B.D., Terrian, D.M., Chappell, W.H., Stivala, F., Libra, M., Martelli, A.M., Steelman, L.S., and McCubrey, J.A. (2008). Targeting prostate cancer based on signal transduction and cell cycle pathways. Cell Cycle *7*, 1745-1762.

Levine, B., Sinha, S., and Kroemer, G. (2008). Bcl-2 family members: dual regulators of apoptosis and autophagy. Autophagy *4*, 600-606.

Li, B., Sun, A., Youn, H., Hong, Y., Terranova, P.F., Thrasher, J.B., Xu, P., and Spencer, D. (2007). Conditional Akt activation promotes androgen-independent progression of prostate cancer. Carcinogenesis *28*, 572-583.

Lockshin, R.A., and Zakeri, Z. (2004). Apoptosis, autophagy, and more. Int J Biochem Cell Biol *36*, 2405-2419.

Luo, J., Solimini, N.L., and Elledge, S.J. (2009). Principles of cancer therapy: oncogene and non-oncogene addiction. Cell *136*, 823-837.

Mahieu, F., Owsianik, G., Verbert, L., Janssens, A., De Smedt, H., Nilius, B., and Voets, T. (2007). TRPM8-independent menthol-induced Ca2+ release from endoplasmic reticulum and Golgi. J Biol Chem *282*, 3325-3336.

Maiuri, M.C., Zalckvar, E., Kimchi, A., and Kroemer, G. (2007). Self-eating and self-killing: crosstalk between autophagy and apoptosis. Nat Rev Mol Cell Biol *8*, 741-752.

Malumbres, M., and Barbacid, M. (2009). Cell cycle, CDKs and cancer: a changing paradigm. Nat Rev Cancer *9*, 153-166.

Matranga, C.B., and Shapiro, G.I. (2002). Selective sensitization of transformed cells to flavopiridol-induced apoptosis following recruitment to S-phase. Cancer Res *62*, 1707-1717.

McDonnell, T.J., Troncoso, P., Brisbay, S.M., Logothetis, C., Chung, L.W., Hsieh, J.T., Tu, S.M., and Campbell, M.L. (1992). Expression of the protooncogene bcl-2 in the prostate and its association with emergence of androgen-independent prostate cancer. Cancer Res *52*, 6940-6944.

Mulholland, D.J., Tran, L.M., Li, Y., Cai, H., Morim, A., Wang, S., Plaisier, S., Garraway, I.P., Huang, J., Graeber, T.G., *et al.* (2011). Cell autonomous role of PTEN in regulating castration-resistant prostate cancer growth. Cancer Cell *19*, 792-804.

Nelson, W.G., De Marzo, A.M., and Isaacs, W.B. (2003). Prostate cancer. N Engl J Med *349*, 366-381.

Nevins, J.R. (2001). The Rb/E2F pathway and cancer. Hum Mol Genet *10*, 699-703.

Noh, K.H., Kang, T.H., Kim, J.H., Pai, S.I., Lin, K.Y., Hung, C.F., Wu, T.C., and Kim, T.W. (2009). Activation of Akt as a mechanism for tumor immune evasion. Mol Ther *17*, 439-447.

O'Reilly, K.E., Rojo, F., She, Q.B., Solit, D., Mills, G.B., Smith, D., Lane, H., Hofmann, F., Hicklin, D.J., Ludwig, D.L., *et al.* (2006). mTOR inhibition induces upstream receptor tyrosine kinase signaling and activates Akt. Cancer Res *66*, 1500-1508.

Pe'er, D., and Hacohen, N. (2011). Principles and strategies for developing network models in cancer. Cell *144*, 864-873.

Sarker, D., Reid, A.H., Yap, T.A., and de Bono, J.S. (2009). Targeting the PI3K/AKT pathway for the treatment of prostate cancer. Clin Cancer Res *15*, 4799-4805.

Senderowicz, A.M. (2000). Small molecule modulators of cyclin-dependent kinases for cancer therapy. Oncogene *19*, 6600-6606.

Senderowicz, A.M. (2003). Novel small molecule cyclin-dependent kinases modulators in human clinical trials. Cancer Biol Ther *2*, S84-95.

Senderowicz, A.M. (2004). Targeting cell cycle and apoptosis for the treatment of human malignancies. Curr Opin Cell Biol *16*, 670-678.

Senderowicz, A.M., and Sausville, E.A. (2000). Preclinical and clinical

development of cyclin-dependent kinase modulators. J Natl Cancer Inst *92*, 376-387.

Shah, M.A., and Schwartz, G.K. (2000). The relevance of drug sequence in combination chemotherapy. Drug Resist Updat *3*, 335-356.

Shen, M.M., and Abate-Shen, C. (2007). Pten inactivation and the emergence of androgen-independent prostate cancer. Cancer Res *67*, 6535-6538.

Stambolic, V., Suzuki, A., de la Pompa, J.L., Brothers, G.M., Mirtsos, C., Sasaki, T., Ruland, J., Penninger, J.M., Siderovski, D.P., and Mak, T.W. (1998). Negative regulation of PKB/Akt-dependent cell survival by the tumor suppressor PTEN. Cell *95*, 29-39.

Sullivan, G.F., Amenta, P.S., Villanueva, J.D., Alvarez, C.J., Yang, J.M., and Hait, W.N. (1998). The expression of drug resistance gene products during the progression of human prostate cancer. Clin Cancer Res *4*, 1393-1403.

Swanton, C. (2004). Cell-cycle targeted therapies. Lancet Oncol *5*, 27-36.

Taylor, B.S., Schultz, N., Hieronymus, H., Gopalan, A., Xiao, Y., Carver, B.S., Arora, V.K., Kaushik, P., Cerami, E., Reva, B., *et al.* (2010). Integrative genomic profiling of human prostate cancer. Cancer Cell *18*, 11-22.

Thorburn, A. (2008). Apoptosis and autophagy: regulatory connections between two supposedly different processes. Apoptosis *13*, 1-9.

Wang, S., Gao, J., Lei, Q., Rozengurt, N., Pritchard, C., Jiao, J., Thomas, G.V., Li, G., Roy-Burman, P., Nelson, P.S., *et al.* (2003). Prostate-specific deletion of the murine Pten tumor suppressor gene leads to metastatic prostate cancer. Cancer Cell *4*, 209-221.

Westin, P., Stattin, P., Damber, J.E., and Bergh, A. (1995). Castration therapy rapidly induces apoptosis in a minority and decreases cell proliferation in a majority of human prostatic tumors. Am J Pathol *146*, 1368-1375.

Wiseman, D.A., Werner, S.R., and Crowell, P.L. (2007). Cell cycle arrest by the isoprenoids perillyl alcohol, geraniol, and farnesol is mediated by p21(Cip1) and p27(Kip1) in human pancreatic adenocarcinoma cells. J Pharmacol Exp Ther *320*, 1163-1170.

Yu, S.G., Hildebrandt, L.A., and Elson, C.E. (1995). Geraniol, an inhibitor of mevalonate biosynthesis, suppresses the growth of hepatomas and melanomas transplanted to rats and mice. J Nutr *125*, 2763-2767.

Zacharatos, P., Kotsinas, A., Evangelou, K., Karakaidos, P., Vassiliou, L.V., Rezaei, N., Kyroudi, A., Kittas, C., Patsouris, E., Papavassiliou, A.G., *et al.* (2004). Distinct expression patterns of the transcription factor E2F-1 in relation to tumour growth parameters in common human carcinomas. J Pathol *203*, 744-753.

Zhou, J., Huang, W., Tao, R., Ibaragi, S., Lan, F., Ido, Y., Wu, X., Alekseyev, Y.O., Lenburg, M.E., Hu, G.F., *et al.* (2009). Inactivation of AMPK alters gene expression and promotes growth of prostate cancer cells. Oncogene *28*, 1993-2002.

# VI. 국문초록

전립선암은 남성 암 발생 증가률 1위를 차지하며 사망으로 만드는 주요 원인 중 의 하나이다. 전립선암에 대한 치료로는 안드로젠 박탈법이 실시되고 있지만 치료를 하더라도 재발하는 환자의 비율이 약 30%로 매우 높다. 결국 호르몬 불응성암으로 발전하게 되고 아직까지 효과적인 치료제가 없다는 점이 큰 문제로 여겨지고 있다.

본 연구에서는 호르몬 불응성암 세포주의 성장 기작을 이해하기 위해 monoterpene compounds를 이용하여 호르몬 불응성암 세포주인 PC-3세포에 처리하였다. 그 결과 AKT경로를 불활성화시키며 성장을 억제시킴을 관찰하였다. 특히 호르몬 불응성암 세포주에서는 발암 억제유전자인 PTEN이 손실되어 있기 때문에 AKT경로가 매우 활성화 되어있다. 그래서 AKT를 표적으로 하면 세포자멸을 기대할 수 있었고, 실험적으로 AKT 억제제에 의해 세포성장이 억제됨을 확인하였다. 하지만 억제된 세포성장 현상과는 상반되게 AKT knockdown 실험에서는 세포성장이 저해되지 못하였다. 게다가 AKT저해는 RTK를 저해하는 음성 되먹임 고리가 완화되기 때문에 AKT저해에 의한 효과를 이해하기 위해 network 분석 방법을 이용하여 AKT와

가까운 hub 단백질인 E2F1을 규명하였다. E2F1은 AKT에 의해 유도되는 증가된 RTK발현을 조절할 수 있기 때문에 E2F1과 AKT를 동시에 knockdown 한 실험에서 세포의 성장이 크게 억제됨을 관찰 할 수 있었다.

지금까지의 실험결과를 통해 AKT와 E2F1의 표적은 전립선 암치료의 새로운 치료제 마커로써 제시될 수 있을 뿐만 아니라 암세포의 성장기전을 이해하는데 있어 중요한 표적으로 이용될 것으로 사료된다.